IMPACT OF CURING TIME ON WARM MIX ASPHALT SHORT-TERM PERFORMANCE

BY

ANGELI MARIZ URBANO GAMEZ

THESIS

Submitted in partial fulfillment of the requirements
for the degree of Master of Science in Civil Engineering
in the Graduate College of the
University of Illinois at Urbana-Champaign, 2012

Urbana, Illinois

Adviser:

Professor Imad L. Al-Qadi

ABSTRACT

The emerging use of warm mix asphalt (WMA) technology has led to economic and environmental benefits for transportation agencies and road users. Among these benefits is the reduced mixing and compaction temperatures of WMA. However, decreased temperatures may affect the resulting complex modulus to withstand traffic loads. A performance evaluation of WMA over various 'curing' periods would determine the evolution of the complex modulus over time. This allows to identify the optimum time for opening WMA paved surfaces to traffic. The effect of curing time on the short-term performance of the warm stone matrix asphalt (warm-SMA), produced with chemical WMA additives, is investigated. The curing periods include: three, six and 12 hours; one, three and seven days; and three, six and 12 weeks.

The main objective of this study is to experimentally characterize the short-term performance of WMA produced with two types of chemical additives: Evotherm^{TM} 3G and Rediset® LQ-1106. The results were analyzed for statistical significance and the effect of warm-SMA on the life cycle cost analysis and life cycle assessment was evaluated. It was determined that the warm-SMA had comparable mechanical properties to the conventional SMA, while providing economic and environmental advantages.

Dedicated in memory of my grandmother, Teodora Gamboa Urbano, who taught me to live every day with a passionate heart and strong-willed mind.

ACKNOWLEDGEMENTS

TABLE OF CONTENTS

CHAPTER 1.   INTRODUCTION

Societal demands for transportation infrastructure have grown immensely over the last several decades. In order to meet the demands, a large amount of materials, energy consumption and monetary investment is essential. However, limited natural resources pose a significant challenge to meet transportation system needs. An optimized solution is sustainability, which can encapsulate economic development and environmental preservation. In order to produce long-lasting and high quality pavements, current pavement design systems can be refined by means of incorporating sustainable and innovative practices.

The transportation industry aimed to combine sustainability with innovation through recycled pavement materials and advanced technologies that promote long-term economic and environmental benefits. Some of the most common sustainable and innovative measures include warm mix technologies, recycled asphalt materials, and stone mastic asphalt mixtures. Although these may be limited to the scope of construction materials, they present themselves as integral parts of pavement preservation and maintenance.

Warm mix asphalt (WMA) is a technology which enables a significant degree of reducing the production and paving temperatures in comparison to hot-mix asphalt (HMA) without compromising the performance characteristics of the asphalt. This reason positively affects an economic standpoint due to the fact that the plant fuel consumption can be reduced by 10-35% *(1)*. In addition, past studies reveal noxious gaseous emissions may be decreased by 15-70% reduction when WMA is utilized *(2)*. Various WMA technologies exist today, including organic, chemical and foaming additives. Typically, WMA additives are introduced in the mixing phase, which alters the characteristic of the conventional HMA through binder viscosity reduction. This chemically altering process promotes an adequate asphalt coating over the aggregates, thereby improving the mixture workability and compaction at lower temperatures.

Moreover, the introduction of recycled asphalt pavement (RAP) into the asphalt concrete mix design has extended sustainability to greater heights, as it decreases the need for virgin material and deters from disposal into landfills. However, due to the material property variations of RAP, which may have been affected by thermal weathering and traffic loading over the pavement's life span, typical percentages of RAP that are used in a conventional mix design seldom increase

over 20 to 25%. Additionally, high percentages of fines in RAP, due to the rough milling mechanism, and the overheating process of virgin aggregates present a significant problem to mixture design and production. Certain measures, such as splitting into stockpiles and fractionation, improve RAP gradation control.

Another recycled material that has been used in asphalt pavements is ground tire rubber (GTR), typically processed from old tires. It can be introduced into the mix design via the wet process (with the asphalt binder) or dry process (with aggregates). Previous studies have indicated that the aromatic oil absorption and rubber particle swelling are processes that have influenced the viscosity growth in GTR-modified asphalt binders, thereby, improving the resistance of the asphalt mixes to rutting. However, instability and separation of the particles pose predominant challenges in using modified asphalt binders.

Lastly, stone matrix asphalt (SMA) concrete is a gap-graded concrete that acquires its structural integrity and strength based upon the coarse aggregate stone-to-stone contact. However, for stability, the asphalt binder is often reinforced with either mineral filler, fibers or stabilizing additive *(3)*. Major positive attributes of the SMA is increased rut and skid resistance, durability, resistance to reflective cracking, improved drainage condition and reduced noise pollution *(4)*.

These mix design modifications have been proven to perform equally well or better than conventional HMA. Therefore, it is only necessary to optimize the current mix design by incorporating various innovative and sustainable design measures, including WMA, RAP, GTR and SMA. Not only do they provide economic relief and promote environmental friendliness, but they exhibit a complimentary relationship. As temperature reduction in WMA leads to less oxidation of the asphalt binder during mixing, the mix may become more susceptible to permanent deformation. In order to counteract this phenomenon, it is deemed appropriate to include RAP, GTR and SMA structure. Furthermore, with the reduced temperature of the WMA, it is a concern if the required complex modulus could be reached upon opening the newly constructed pavement to traffic. In this research study, various curing periods are investigated to determine how chemical WMA additives affect the short-term mechanical properties of the mixture. A careful laboratory investigation and careful consideration to evaluate the warm-SMA, containing RAP and GTR modified binder, are presented in this study.

In order to create a robust evaluation of the material, the life cycle cost analysis and life cycle assessment are appended to explore the economic and environmental impact factors of the optimized sustainable mixture.

1.1 Background of Warm Mix Asphalt

Warm-mix asphalt is an emerging technology that began in the mid-90's to allow for lower asphalt concrete mixing and compaction temperatures in comparison to the conventional HMA. Initially developed in Europe, the United States has continued to explore the material performance and benefits of WMA. Typically, the mixing and compaction temperatures for HMA range from 150 to 180 ^{o}C (300 to 350 ^{o}F). However, past studies have revealed that it could be decreased to as low as 100 to 140 ^{o}C (212 to 280 ^{o}F) for WMA *(2)*. In addition, HMA often constitutes for high energy consumption and significant production of greenhouse gases and hazardous fumes. Using WMA may address the environmental issues, reduce stack emissions and energy consumption, and possibly achieve improved workability and compatibility *(5)*.

Additional potential benefits of WMA include improved asphalt mixture compaction, increased use of reclaimed asphalt pavement (RAP), extended paving season, reduced oxidative hardening, and reduced worker exposure to noxious fumes. Despite its potential benefits, the durability and performance issues of WMA have been brought into question due to the lack of long-term field data. Warm-mix asphalt may also become more susceptible to permanent deformation and can possibly be distorted under early-age traffic since the production temperatures are decreased. Another issue is the possibility of incomplete evaporation of the aggregate moisture since the aggregates are heated at a lower temperature, thereby possibly increasing the moisture damage susceptibility of the WMA.

To evaluate the performance of WMA, many studies have been conducted *(6-12)*. Most of these studies reported equivalent performance of WMA with respect to HMA. However, it should be considered that the performance of the WMA is highly dependent on the technology used to produce the WMA. Currently, more than 20 WMA technologies are marketed in the United States *(13)*. Due to different working mechanisms, WMA prepared with various techniques may provide different short-term and long-term performances. Therefore, before one decides which

WMA additive to use in the field, it is vital to establish a full material characterization and verify the performance by means of comprehensive laboratory testing.

1.2 Problem Statement

Although WMA technology enables the reduction of mixing and compaction temperatures, it has been a concern if the decreased temperatures may affect the resulting complex modulus to withstand traffic loading once the pavement is opened to traffic. A performance evaluation addressing different 'curing' periods of the WMA is needed to determine the evolution of the complex modulus over time. This allows to identify the optimum time for opening WMA paved surfaces to traffic. Therefore, the effect of curing time on the short-term performance of the warm-SMA, produced with chemical WMA additives, is investigated.

1.3 Research Objective

The main objective of this study is to experimentally characterize the short-term performance of WMA produced with two types of chemical additives, namely Evotherm^{TM} 3G and Rediset® LQ-1106. To achieve this objective, the following research tasks were conducted:

1) Evaluation of the early-age mechanical properties of WMA with respect to HMA through laboratory performance tests. Extensive laboratory tests were conducted on a control SMA and two warm-SMAs produced with Evotherm^{TM} 3G and Rediset® LQ-1106 additives. The tests included complex modulus, flow number, loaded wheel track, indirect tensile (IDT) strength, and semi-circular bending (SCB) fracture, and;

2) Investigation of the curing time effect on various mechanical properties of WMA based on the laboratory test results. For all the SMA mixtures, performance tests were conducted at various curing periods between three hrs and seven days after compaction. Given that the fracture property is not initially time-critical; the SCB fracture tests were conducted at various curing times between one day and 12 weeks after compaction.

1.4 Scope of Study

A comprehensive literature review of the WMA technologies, SMA, RAP and GTR modified binder was completed in order to evaluate the advantages and challenges of each material. Only the chemical WMA additives were investigated to create a primary focus on the performance of the warm-SMA combined with RAP and GTR-modified binder in comparison to a control SMA and to determine the effect of varied curing periods of three, six and 12 hours; one, three and seven days; and three, six and 12 weeks. The mixtures were then investigated under mechanical characterization tests including the complex modulus, loaded-wheel track, flow number, indirect tensile strength and semi-circular bending. Furthermore, a life cycle assessment and life cycle cost analysis were performed to determine the environmental and economic impacts of the modified asphalt mixture. Finally, conclusions were drawn and recommendations for future research relating to the study were presented.

CHAPTER 2.   CURRENT STATE OF KNOWLEDGE

2.1 Warm Mix Asphalt Additives

Many WMA additives have been developed in order to either reduce the asphalt binder's effective viscosity or improve mixture workability and compatibility at a reduced temperature than the conventional HMA. Three of the most common WMA technologies that are used include organic or wax additives, chemical additives, and foaming techniques.

2.1.1 Organic Additives

Organic or wax additives are typically used to reduce the viscosity of the asphalt binder at temperatures over 90 ^{o}C (194 ^{o}F). The process demonstrates the decrease in viscosity above the melting point of the wax. Therefore, it is essential to select the type of wax carefully in order to ensure that the melting point of the wax is greater than the expected in-service pavement temperature, due to the possibility of permanent deformation at high temperatures, and to prevent embrittlement of the asphalt binder at low temperatures.

Three of the most commonly used organic additives are Sasobit, Asphaltan-B and Licomont BS 100. Sasobit, typically used in the United States, is a Fischer-Tropsch wax, which is a paraffin wax that is produced through hot coat treatment using steam in the presence of a catalyst (Figure 2.1). It is a fine white crystalline granulate that contains long aliphatic hydrocarbon chains. Often described as an "asphalt flow improved," it has the ability to decrease the viscosity of the asphalt binder and the mixing temperature by 18 to 54 ^{o}C (32 to 97 ^{o}F) *(6)*. Additionally, at a temperature below its melting point, Sasobit forms a crystalline network which increases the stability of the asphalt binder by means of increasing the viscosity of the asphalt binder.

Figure 2.1. Sasobit flakes (left) and prills (right) (*11*).

On the other hand, Asphaltan-B and Licomont BS 100 are not typically used in the United States. Asphaltan-B is a Montan wax that is blended with a fatty acid amide. According to researchers, Montan wax is a culmination of non-glyceride long-chain carboxylic acid esters, free organic acids, alcohols, ketones, hydrocarbons and resins. It is typically produced through the process of solvent extraction of lignite or brown coal, which is used to create car and shoe polishing waxes, and lubricants for molding items. Similar to Sasobit, Asphaltan-B is available in granular or pellet form and is generally mixed with the asphalt binder, allowing for 20 to 30 ^{o}C (68 to 86 ^{o}F) temperature reductions. Licomont BS 100 is a fatty acid amide that is produced by the amine-fatty acid reaction. Another typical way of using this product, besides as a WMA additive, includes asphalt roofing (*2*).

Many researchers have determined that although organic additives improve permanent deformation resistance at high in-service temperatures, wax tends to stiffen the asphalt concrete mixture at ambient or low temperatures which decreases the fracture resistance of the material.

2.1.2 Chemical Additives

Chemical additives differ from organic additives in a way that instead of typically lowering the asphalt binder viscosity, an interfacial reaction between the aggregate and asphalt binder occurs. The frictional forces at the aggregate-binder interface are decreased over a range of temperatures, typically between 85 to 140 ^{o}C (185 to 284 ^{o}F). Chemical additives include a combination of emulsions, surfactants, and polymers to improve aggregate coating and mixture

workability and compaction. It is often used by means of an emulsion or it can be added to the asphalt binder. Typical chemical additives include Evotherm[TM] and Rediset® *(14)*.

Evotherm[TM], developed by MeadWestvaco, is an emulsion with a chemistry package that contains a relatively high asphalt residue of approximately 70%, which is mixed with heated aggregates to produce a mixing temperature between 85 to 115 ^{o}C (185 to 239 ^{o}F). Although water is introduced into the mixture due to the emulsion process, most of the water particles evaporate or flashes off as steam when introduced onto the heated aggregates. A relatively newer technology has emerged, which is called the dispersed asphalt technology (DAT), wherein the same chemical composition is diluted with a small amount of water that is injected into the asphalt binder line prior to the mixing chamber, containing the aggregates. However, a major challenge with this water-based chemical additive is moisture susceptibility if the total amount of water is not completely evaporated, which can lead to stripping or weak aggregate-binder interface. This led to the creation of the newest generation, Evotherm[TM] 3G (Figure 2.2). It is a water-free chemical package that contains surfactant and anti-stripping agent to improve aggregate coating, workability and compaction. Using the Evotherm[TM] 3G, the mixing temperature can be lowered by 35 to 45 ^{o}C (60 to 85 ^{o}F).

Figure 2.2. Evotherm[TM] 3G WMA additive.

Similarly, Rediset® LQ, (Figure 2.3) developed by AzkoNobel Surface Chemistry LLC, is a chemical additive that allows mixing temperatures to be reduced by 15 to 30 ^{o}C (25 to 55 ^{o}F) and provides a built-in anti-stripping effect. It contains surfactants that reduce the surface tension of

the asphalt binder, enabling an improved aggregate coating on the aggregate surface. The typical dosage that is used may increase to as high as 0.75% by the weight of the asphalt binder. The addition does not change the performance grade of the binder. The modified binder has a higher affinity to the aggregate's surface in contrast to water, which bonds the binder onto the aggregate surface, despite if the aggregate is not completely dry.
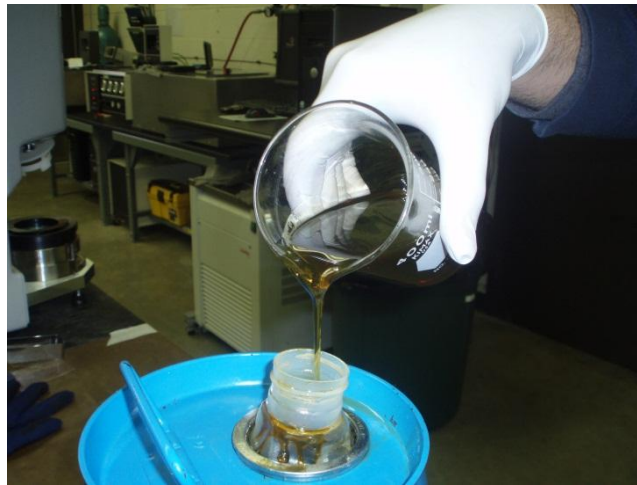
Figure 2.3. Rediset LQ-1106 WMA additive.

2.1.3 Foaming Techniques

The last major type of WMA additive is foaming additive. It is a process that introduces water into the hot asphalt binder, either by means of a foaming nozzle or using a hydrophilic material, such as zeolite or damp aggregates. As the water gets in contact with the hot asphalt, water turns into steam at atmospheric pressure, expanding by a factor of 1,673 *(2)*. Rapid evaporation of water by injecting cold water into the heated asphalt binder increases the volume of the asphalt binder and reduces its viscosity for a short period to promote full coating of the aggregates at a lower temperature than HMA. One major concern with this method is the presence of water; therefore, at times anti-stripping agents are added in order to reduce the moisture damage susceptibility. Typical foam techniques include Aspha-min, Low-Energy Asphalt, Double Barrel Green, Synthetic Zeolite, and WAM-Foam *(14)*.

2.2 Recycled Asphalt Pavement in WMA

A multitude of asphalt pavements across the United States have reached their pavement service lives and have been transferred to waste landfills. However, in order to alleviate the

amount of excavated asphalt concrete in landfills, many researchers and agencies have implemented the use of RAP in asphalt mixtures, at times up to 50%. Although this emerging practice promotes environmental friendliness, it is vital to push the envelopes of pavement engineering towards greater sustainability. Therefore, it is only appropriate to combine two sustainable methods, RAP and WMA.

Several studies have been conducted regarding the properties and performance of RAP, including the chemical composition of the already aged and stiffened RAP binder *(15-23)*. In general, past research studies determined that the use of RAP would increase the overall stiffness of the asphalt concrete mixture. The increased stiffness of the mixture with RAP could promote rutting resistance; however it could also exacerbate low-temperature cracking potential, as asphalt concrete exhibits a brittle behavior at low temperatures. Therefore, in order to limit further aging of the RAP and improve workability, researchers evaluated the combination of WMA and RAP *(24)*. Shu et. al *(25)* and Tao *(26)* determined that WMA with RAP had a higher tensile strength in comparison to HMA and reduced post-failure tenacity in comparison to HMA containing RAP. Wen and Kim *(27)* found that the fracture energy was highly correlated with field fatigue performance and that mixtures with higher fracture energy have less fatigue cracking.

Additionally, due to the uneven milling process of RAP, there is a high variability in the gradation of the material (Figure 2.4). One process that can control variability is through fractionation, wherein the collected RAP undergoes gradation analysis.

Figure 2.4. Varied RAP gradation (*28*).

2.3 Ground Tire Rubber Modified Asphalt Binder

The storage, disposal and recycling of used tires has been a significant concern for agencies across the nations. Due to the physical bulkiness of the tires, old tires tend to take up 75% of landfill space. Therefore, in order to alleviate this issue, the use of ground tire rubber (GTR) as an asphalt mixture constituent has been considered and/or implemented (Figure 2.5).

Figure 2.5. Ground tire rubber stockpile (*29*).

Incorporating GTR into the asphalt binder not only enables a way to recycle scrap tires but it can also introduce a potential improvement to the physical characteristics of the asphalt binder in

regards to rutting resistance, road noise reduction, aging and fatigue resistance and thermal cracking *(30-32)*. Tires are typically composed of complex vulcanized rubber, which includes natural rubber (like polysioperence) and synthetic rubber (like styrene-butadiene), which are cross-linked with sulfur and reinforced with carbon black. Similar to asphalt binder, tire rubber is a colloidal material that can be divided into saturates, aromatics, resins, and asphaltenes *(33)*. With similar chemical composition, it is deemed that the interaction between the GTR and asphalt binder is more of an exchange of material characteristics without significant chemical alterations of each component *(34, 35)*.

However, based on previous studies, it was determined that high temperature and mixing rate could induce a significant effect on the material interaction. Ground tire rubber particles can dissolve more in softer asphalts that have lower performance grades than stiffer asphalt. This can be related to the higher rate of diffusion of the softer asphalt into the GTR structure *(36-38)*. Additionally, increase in the shearing rate could imply mechanical energy transfer into the GTR and increase in the diffusion rate of the asphalt mixture into the structure, which leads to degradation of the GTR into the asphalt matrix. With the addition of GTR into the asphalt mixture, the mixing and compaction temperature are deemed to increase. Therefore, in order to offset the increased mixing and compaction temperature, the addition of WMA additives could lower the temperatures and produce mechanical characteristics that would be comparable to the conventional HMA.

2.4 Stone Matrix Asphalt

Originally produced in Germany during the 1960s, stone matrix asphalt (SMA) is a gap-graded asphalt mixture, which acquires its stability from the stone skeleton (stone-to-stone contact) of the coarse aggregates (Figure 2.6). The complex network of the coarse aggregate interlock provides high shearing resistance and efficient load distribution throughout the aggregate structure. Rich mastic, which is comprised of asphalt binder, small percentage of fine aggregates and stabilizing additive (and/or fiber), hold the coarse aggregate structure together.

Figure 2.6. SMA coarse aggregate skeleton.

The relatively high-shear strength resistance of SMA results in reducing its permanent deformation potential. Hence, the rehabilitation cost of the pavement is lowered during its service life. In particular, the Illinois State Highway Tollway Authority (ISHTA) determined that the use of SMA in full-depth asphalt concrete pavements could increase pavement service life by 30 to 40% compared to typical HMA service life of 10 to 20 years. This can very well be correlated to the capability of the coarse aggregate skeleton to withstand heavy traffic loads in comparison to the fine aggregate asphalt mastic of HMA (*1*).

Furthermore, previous research studies determined that SMA promotes surface friction, durability, reflective cracking resistance, better drainage condition and reduced noise pollution *(4)*. However, due to the gap-graded nature of the SMA, a relatively high asphalt binder content is required, typically ranging from 5.5 to 7.5%, and stabilizing fibers or polymers are used to prevent binder drain down *(39, 40)*. Therefore, agencies tend to be mindful of optimizing the economic impact of the SMA's stabilized skeleton and need for higher binder content.

The use of WMA additive, RAP, and GTR in SMA demonstrates innovation and sustainability. The following chapter presents the laboratory investigation of the testing materials.

CHAPTER 3. TESTING MATERIALS

In order to fully comprehend asphalt concrete behavior, the material was investigated at the component level. Generally, asphalt concrete materials could be divided into two main categories, namely, asphalt binder and aggregates. With regards to the asphalt binder including GTR, the performance grading (PG) specifications were used. The aggregate gradation analysis was conducted to ensure that the combination of the SMA coarse aggregates, fractionated RAP (FRAP) and mineral filler was compliant with the mix design specifications.

3.1 Ground Tire Rubber Modified Asphalt Binder

The GTR modified asphalt binder was investigated to ensure material property compliance with the Illinois State Highway Toll Authority (ISHTA) specifications. It is worth noting that due to the addition of GTR with the asphalt binder, the performance grade of the modified binder resulted to PG 76-22. Additional Illinois Department of Transportation (IDOT) performance grading requirements were performed to accommodate the modified asphalt binder, including the screen and separation of polymer test. The following table indicates that the property testing results of the GTR-modified asphalt binder conformed to the ISHTA specifications.

Table 3.1. Property testing results of PG64-22 with 12% GTR.

Property		AASHTO Test Method	Specs* IL Tollway	Results
Original Binder				
Appearance	Homogeneity/Setting	Observation	Report	Non homogeneous
	Smoothness			Not smooth
Flash Point, ^{o}C (^{o}F)		T 48	230 min	288 (550)
Screen Test, Lumps/particles		IL DOT (Note #1)	None	45% GTR particles on screen
Viscosity, Pa*s	135 ^{o}C	T 316	3.0 max	2.736
Separation of Polymer, ^{o}C (^{o}F)	Top	IL DOT (Note #2)	Report	56.40 (133.50)
	Bottom			56.25 (133.25)

Table 3.1. (continued) Property testing results of PG64-22 with 12% GTR.

Property		Difference / Temp	Test	Specification	Result
		Difference		2 (4) max	0.15 (0.25)
Force Ratio, f1/f2, 500 mm/min, 300 mm elongation		4 ^{o}C	T 300	0.35 min	Break at 250 mm
Dynamic Shear, kPa (G*/sinδ, 10 rad/sec)		76 ^{o}C	T 315	1.0 min	1.908
Phase Angle, δ (^{o}C)				Report	73.6
After RTFOT					
Mass Change, % (Mass Loss is reported as negative)			T 420	1.0 max	-0.14
Dynamic Shear, kPa (G*/sinδ, 10 rad/sec)		76 ^{o}C	T 315	2.2 min	4.439
Phase Angle, δ (^{o}C)				Report	65.7
Elastic Recovery, % (10cm elongation)		25 ^{o}C	ASTM D 6084(A)	70 min	74
MSCR, % Recovery	100 Pa	76 ^{o}C	TP 70-07	Report	47.9
	3,200 Pa				8.7
Jnr, Pa^{-1}	3,200 Pa				2.36
Pressure Aging Residue (100 ^{o}C, 2070 kPa, 20 hrs)					
Dynamic Shear, kPa (G*/sinδ, 10 rad/sec)		31 ^{o}C	T 315	5,000 max	1.21
Phase Angle, δ (^{o}C)				Report	42.6
Creep Stiffness	Stiffness, MPa (60 sec)	-12 ^{o}C	T 313	300 max	82
	m value			0.300 min	0.328

Conversion: ^{o}C = (5/9) (^{o}F - 32); 1 psi = 6.9 kPa

* Specification for PG76-22

Note#1: IDOT Bituminous Materials Test Procedure, "Screen Test." The GTR modified binder was sieved to determine the percentage of solid particles.

Note#2: IDOT Test Procedure, "Separation of Polymer from Asphalt Binder." Difference in temperature of the softening point between top and bottom portions was obtained.

3.2 Stone Mastic Asphalt Mixture Design

A 12.5 mm (0.5 in) SMA design, typically used by Chicago area contractors on large-scale expressway overlay projects, was selected as the control mixture for the research study. The two WMA evaluated were prepared with the addition of 0.5% Evotherm^{TM} 3G and 0.5% Rediset® LQ-1106 by the weight of asphalt binder to the control SMA.

Table 3.2. Comparison of control SMA and warm-SMAs.

Mix	N_{des}	NMAS (mm)	Binder	Fine FRAP	WMA Additive	Compaction Temperature (^{o}C)
Control SMA					NA	152
Evotherm^{TM} 3G SMA	80	12.5	6% PG 64-22 with12% GTR	8%	0.5% of binder	127
Rediset® SMA					0.5% of binder	127

As indicated in Table 3.2 the control SMA is a binder-lift mix with the nominal maximum aggregate size (NMAS) of 12.5 mm (0.5 in) and 6% total asphalt binder content. According to ISHTA, a PG64-22 asphalt binder that is combined with 12% ground tire rubber (GTR) bumps the actual performance grade of the binder to PG76-22. It also contains 8% fine fractionated recycled asphalt pavement (FRAP), which has been obtained from the I-290 resurfacing project. The compaction temperature for the control SMA is determined to be 152 ^{o}C (305 ^{o}F), whereas the compaction temperature for the two warm-SMAs with Evotherm^{TM} 3G and Rediset® is 127 ^{o}C (260 ^{o}F). The gradation of the control SMA is shown to be in compliance with the limits as shown in Figure 3.1.
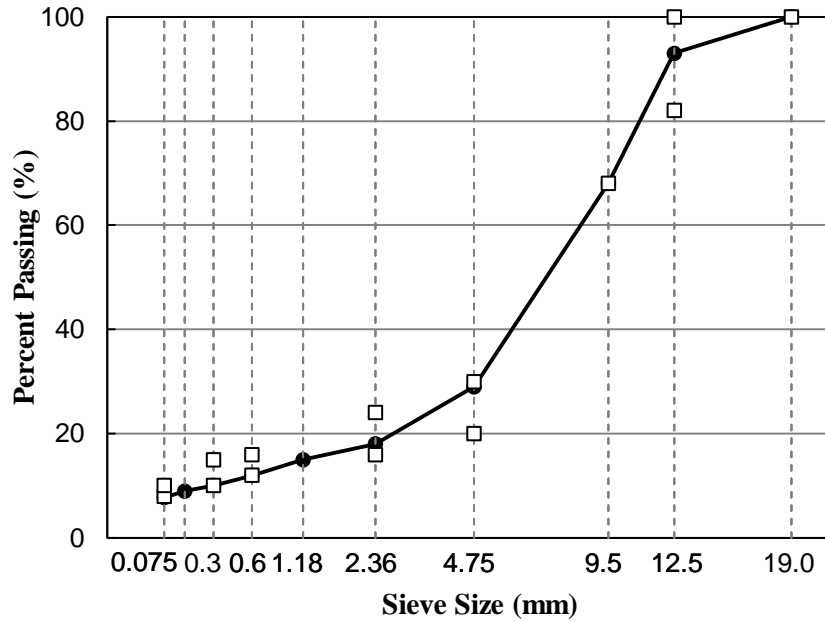
Figure 3.1. Gradation of control SMA.

3.3 Specimen Preparation

The materials, including the aggregates, FRAP, mineral filler, asphalt binder and Evotherm^TM 3G additive were obtained from the Geneva Construction plant in the Chicago area in order to conduct laboratory-mixed and laboratory-compacted (LMLC) specimens. Additionally, the Rediset® LQ-1106 additive was provided by AzkoNobel. For the control SMA, both the batched aggregates and asphalt binder were heated at the mixing temperature for three hrs prior to mixing (Table 3.3). Figure 3.2 illustrates sets of batched aggregates, including FRAP and mineral filler, prior to heating to the appropriate mixing temperature.

17

Figure 3.2. Batched SMA aggregates with FRAP and mineral filler.

It is noteworthy that for the two warm-SMAs with Evotherm[TM] 3G and Rediset®, the batched aggregates were heated at lower temperatures in comparison to the control SMA, due its lower mixing temperature requirement. Additionally, the asphalt binder was heated to the designated temperature for 2.5 hrs prior to the addition of the WMA additive to the binder using a dropper (Figure 3.3).

Figure 3.3. Addition of the chemical WMA additive to asphalt binder.

The additive was then immediately blended with the binder using a low-shear mixer for five minutes while the binder was placed on top of a hot plate (Figure 3.4). After the additive was completely blended with the binder, it was placed back into the oven at the mixing temperature for 0.5 hr. For each specimen, temperatures of the aggregates and binder were verified using

thermometers in order to ensure that the target mixing temperature was reached prior to the mixing phase. It should be noted that the SMA containing WMA additive, will be denoted as 'warm-SMA' in the following sections.
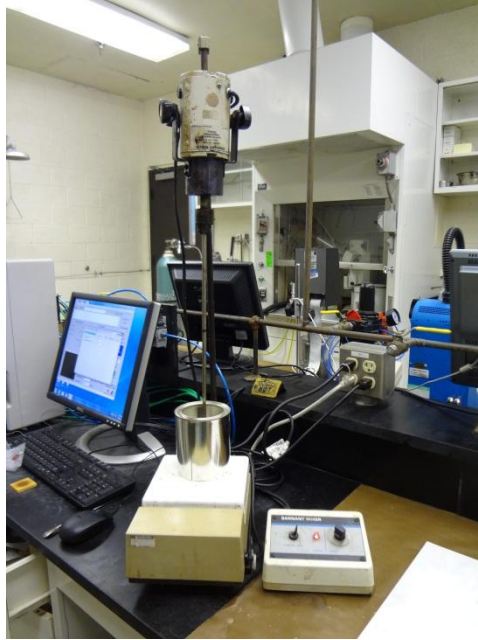

Figure 3.4. Blending the chemical WMA additive and binder using a low-shear mixer.

After mixing was completed, both the control SMA and the two warm-SMAs were conditioned at their respective compaction temperatures, as presented in Table 3.3, for two hrs. This would simulate the short-term aging in the field during production and placement. A portable gyratory compactor, as shown in Figure 3.5, was utilized to compact all the testing specimens. The appropriate dimensions and number of gyratory specimens for each test are listed in Table 3.4. After compaction, all gyratory specimens were initially cooled down using a fan and then stored in an environmental room at 25 ^{o}C (77 ^{o}F) until they were tested at the desired curing time.

Table 3.3. Mixing and compaction temperatures for each mixture.

Mix	Mixing Temperature (^{o}C)*	Compaction Temperature (^{o}C)
Control SMA	163	152
Evotherm^{TM} 3G SMA	138	127
Rediset® SMA	138	127

*Temperature Conversion: ^{o}C = (5/9) (^{o}F - 32)

Figure 3.5. Portable gyratory compactor for specimen preparation.

Table 3.4. Dimension and number of the gyratory and testing specimens.

Test	Complex Modulus	Flow Number	Loaded Wheel Track	IDT	SCB
Gyratory Specimen Dimension (mm)	150 (D^1) 170 (H^2)	150 (D) 170 (H)	150 (D) 130 (H)	150 (D) 150 (H)	150 (D) 150 (H)
# of Gyratory Specimens for Each Test	3	3	2	1	1
Testing Specimen Dimension (mm)	100 (D) 150 (H)	100 (D) 150 (H)	62 (H)	150 (D) 50 (H)	75 (R^3) 50 (H)
# of Testing Replicates for Each Test	3	3	2	2	4

[1]Diameter; [2]Height; [3]Radius

Conversion: 1 mm = 0.04 in

CHAPTER 4.   RESEARCH APPROACH

The laboratory program included the complex modulus, flow number, loaded-wheel track, indirect tension and semi-circular bending. Three asphalt mixtures, namely a control SMA, and two warm-SMAs prepared with Evotherm^{TM} and Rediset®, were investigated under various curing periods: three, six and 12 hours; one, three and seven days; and three, six and 12 weeks.

4.1 Complex (Dynamic) Modulus Test

For linear viscoelastic materials, the complex modulus describes the stress-strain relationship under sinusoidal loading in the frequency domain. It is a true complex number, containing both a real and imaginary component of the modulus that is typically identified by E*, which can be defined as the ratio of the amplitude of the sinusoidal stress, at any given time and angular loading frequency, over the sinusoidal strain, at the same time and frequency, resulting in a steady-state response. By taking the absolute value of the complex modulus, the dynamic modulus can be defined. It can be calculated using the ratio between the peak steady-state stress over the peak steady-state strain (Figure 4.1). A lag between the peak stress and strain is defined to be the phase angle, ϕ. For a purely elastic material, ϕ is equal to zero, whereas, for a purely viscous material, ϕ is equal to 90°.

Figure 4.1. Complex modulus setup with extensometers attached onto the specimen.

The dynamic modulus test was conducted using a uniaxially applied sinusoidal stress pattern in accordance with the AASHTO TP-62, "Determining Dynamic Modulus of Hot-Mix Asphalt Concrete Mixtures" *(41)*. The test setup is shown in Figure 4.1. For each mixture and curing period, three replicates were prepared for testing. The test was conducted at room temperature (25 °C or 77 °F) with varying frequencies of 25, 10, 5, 1, 0.5, and 0.1 Hz. However, in comparison to the typical method of testing, by which the master curve spans over multiple temperatures and loading frequencies, the research study was concentrated to be tested at room temperature in order to determine the instantaneous dynamic modulus. The measured dynamic modulus for each test was determined using the following equations:

$$|E*| = \frac{\sigma_0}{\varepsilon_0}$$

(4.1)

$$\sigma = \sigma_0 \sin(\omega t)$$

(4.2)

$$\varepsilon = \varepsilon_0 \sin(\omega t - \phi)$$

(4.3)

where,

$|E*|$ is dynamic modulus;

σ_0 is applied steady state stress amplitude;

ε_0 is measured strain amplitude;

ω is angular frequency ($2\pi f$, where f = frequency); and

ϕ is phase angle in radians ($\omega \Delta t$, where Δt = time lag between stress and strain).

4.2 Loaded-Wheel Track Test

Another test method used to determine the permanent deformation performance of asphalt mixtures was the Hamburg-type loading wheel track tester, manufactured by PMW, Inc (Figure 4.2). The tests at various curing periods were conducted in accordance to the Texas Department of Transportation procedure *(42)*. However, the testing procedure was modified to a dry condition testing at 30 °C (86 °F) to simulate the short-term performance immediately after construction and to allow testing within a short duration of time. This was done to accommodate

the low end of the curing period spectrum, including three, six and 12 hrs, and one and three days.

The test was performed by rolling a 738 N (158 lbs) steel wheel on the specimen surface at 50 passes per minute and stopping after 20,000 passes. Linear variable differential transformers (LVDTs) on each wheel were also calibrated in order to ensure the accuracy of the rut depth measurements. The rut depth at a specified number of wheel passes and the number of passes until failure were both reported. For each mixture and curing period, two pairs of replicates were prepared for testing. After the dry-conditioned tests at various curing periods were completed, specimens cured for seven days were tested under the standard condition (wet and 50 ^{o}C / 122 ^{o}F) to check the rut depth conformance with the Illinois Department of Transportation specifications.

Figure 4.2. Hamburg loaded-wheel track test setup under dry and heated conditions.

4.3 Flow Number Test

The flow number defines the point at which the tertiary flow occurs over a cumulative permanent strain curve that is obtained after the test. It can be determined by locating the minimum value of the strain rate *(43)*. A typical plot of the permanent strain versus loading cycle on a log-log scale is illustrated in Figure 4.3.
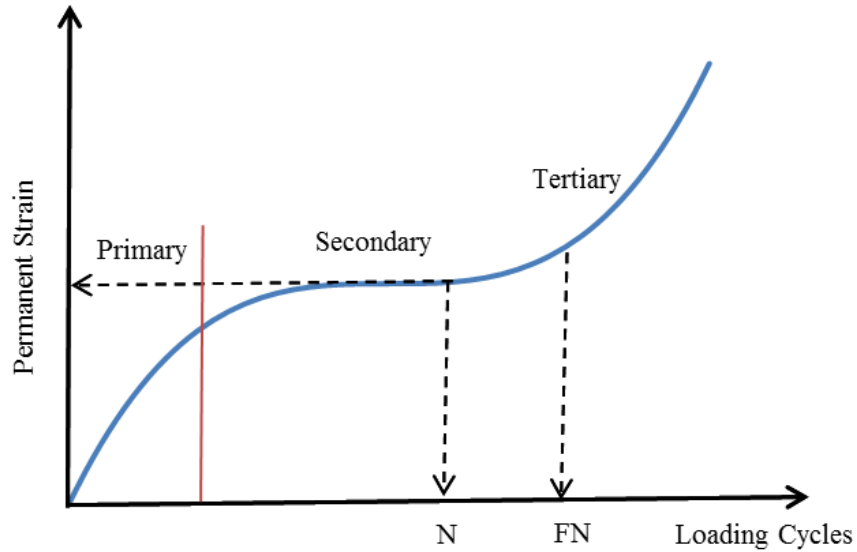
Figure 4.3. Typical flow number test curve that indicates the primary, secondary and tertiary stages of permanent deformation.

Based on the National Cooperative Highway Research Program (NCHRP) Report 465, the flow number can be used as a performance indicator regarding the permanent deformation, or rutting, potential of the mixture under a triaxial repeated load test. The load cycle is comprised of a 0.1 s haversine pulse load and a 0.9 s rest period, which is performed repeatedly to a typical duration of three hrs or 10,000 loading cycles *(43)*. The resulting cumulative permanent deformation curve may then be divided into three regions: primary, secondary and tertiary. The permanent deformation rates decrease in the primary stage and increase again in the tertiary stage. In the tertiary stage, the permanent deformation increases rapidly. The flow number is defined as number of loading cycles at the beginning of the tertiary stage.

In this study, the flow number test was conducted using a uniaxial compressive loading without confinement at 58 °C (136 °F) (Figure 4.4). A loading stress level of 200 kPa (29 psi) was selected in order to reach tertiary flow with a reasonable number of cycles. The test was conducted up to 10,000 cycles or until 5% of cumulative permanent strain was achieved. Based on Dongré et al. *(44)*, the Francken model was used to fit the measured permanent strain as a function of the number of loading cycles.

Figure 4.4. Flow number test setup.

It is a combination of power law function and exponential function, as shown in Equation 4.4. The first derivative of the Francken model is calculated as the rate of permanent strain, whereas the second derivative of the Francken model is calculated to obtain the slope of the rate of permanent strain (Equation 4.5). The flow number is then calculated at the point where the slope of the rate of permanent strain changes direction (from negative to positive).

$$\varepsilon_p = AN^B + C(e^{DN} - 1)$$

(4.4)

$$\frac{\partial^2 \varepsilon_p}{\partial N^2} = AB(B-1)N^{(B-2)} + CD^2 e^{DN}$$

(4.5)

where,

ε_p is accumulated permanent strain;

N is number of loading cycles; and

A, B, C, and D are fitting parameters.

4.4 Indirect Tensile Creep and Strength Test

Creep compliance is a viscoelastic material behavior that can be obtained by dividing the time-dependent strain by the constant applied stress. Tensile strength testing, on the other hand, evaluates the indirect tensile strength of the loaded specimen until tensile failure occurs. The indirect tensile (IDT) creep and strength tests were performed in accordance with AASHTO T-

322-07, "Standard Method of Test for Determining the Creep Compliance and Strength of Hot-Mix Asphalt (HMA) Using the Indirect Tensile Test Device" *(42)*, utilizing a universal testing machine manufactured by Instron®, Inc (Figure 4.5).

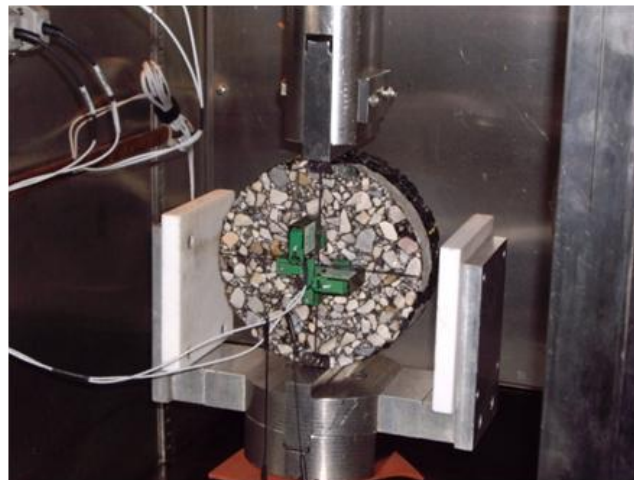**Figure 4.5. Test device used for the indirect tensile test, manufactured by Instron, Inc.**

Figure 4.6. IDT test setup using the Instron machine.

As illustrated in Figure 4.6, a compressive load was applied and the corresponding vertical and horizontal deformations were measured on the two sawn, parallel faces of the specimens using four extensometers, wherein two were placed on each face. The level of loading was adjusted to

ensure that the responses were within the linear viscoelastic strain range. The test was performed at a temperature 10 °C (50 °F) warmer than the low PG of the asphalt binder. The applied loading rate was 0.7 mm/min (0.03 in/min). For each mixture and curing period, two replicates were prepared. For the indirect tensile strength test, the test specimen was loaded until failure at a rate of 12.7 mm/min (0.5 in/min) at room temperature (25 °C or 77 °F). The maximum load that the specimen could bear was recorded to calculate the IDT strength, as indicated in the following equation:

$$S_t = \frac{2P}{\pi \cdot d \cdot b}$$

(4.6)

where,

S_t is tensile strength;

P is maximum applied load;

d is diameter of specimen; and

b is thickness of specimen.

4.5 Semi-Circular Bending Fracture Test

The semi-circular bending (SCB) fracture test was initially proposed by Chong and Kurrupu *(45)* in order to characterize the fracture resistance of asphalt mixtures. Previous studies concluded that fracture energy can be used to differentiate asphalt mixtures with regards to their low-temperature performance. Generally, it could be assumed that the lower the temperature, the lower the fracture energy. The SCB test could also be used to investigate the pure mode I stress intensity factor, since the angle of the notch with respect to the line of loading is zero.

Specimens were cut into semi-circular shaped specimens with a thickness of 50 mm (2 in). A 15 mm (0.6 in) notch was introduced in the middle of the flat section of the specimen to initiate the point of the predetermined crack or failure area. The test was performed at a temperature of -12 °C (10 °F), which is 10 °C (18 °F) warmer than the low-temperature binder performance grade. An illustration of the SCB test setup is shown on Figure 4.7. Using a constant crack mouth opening displacement (CMOD) rate mode, the load, displacement, and CMOD were recorded. The work of fracture was calculated from the SCB test by integrating the load-CMOD curve using the following equation:

$$W_f = \int P du$$

where,

W_f is work of fracture;

P is applied load; and

u is CMOD.

The fracture energy was obtained by dividing the work of fracture by the fractured area.

Figure 4.7. Failed SCB test specimen.

CHAPTER 5. TEST RESULT ANALYSIS AND DISCUSSION

5.1 Performance Evaluation

In order to determine the representative performance of the SMA, various laboratory tests were performed to evaluate the mechanical properties, including the dynamic modulus, flow number, permanent deformation, indirect tensile strength and creep, and fracture property. The mechanical properties of an asphalt mixture were affected by numerous factors, namely, aggregate type and gradation, asphalt binder grade, compaction temperature, curing and aging, anti-stripping treatments, and volumetric parameters. The laboratory test results were used to study the performance of the SMA and the effect of the two WMA chemical additives, which were mixed and compacted at lower temperatures than the control SMA.

The following section explains in details the analysis of the aforementioned testing regime to investigate the effect of mixture property variation and curing time.

5.1.1 Air Void Content

All laboratory specimens were compacted to the target air void content of 6.0% in order to minimize the effect of varying air void content on the mixture performance. As indicated in the given table, the air void content resulted in the range of 6.0 ± 0.5% while the maximum coefficient of variation (COV) was 6.0% (Table 5.1). This implies a reasonable repeatability using the portable gyratory compactor and negligible effects of the slightly varied air void contents.

Table 5.1. Air void contents for testing specimens (%).

Mixture	Complex Modulus		Loaded Wheel Track		IDT		SCB	
	Average (%)	COV (%)	Average (%)	COV (%)	Average (%)	COV (%)	Average (%)	COV (%)
Control SMA	5.9	3	6.2	2	6.0	3	6.0	3
Evotherm^{TM} 3G SMA	6.0	3	5.7	6	6.3	4	6.3	2
Rediset® SMA	6.2	6	5.7	5	6.3	3	6.2	5

5.1.2 Dynamic Modulus

The dynamic modulus test protocol has been modified to limit the data acquired from a set of five temperatures into one, which is room temperature. The main point of concern of this research study is to determine the material behavior immediately when the pavement can be opened to traffic with varying curing times.
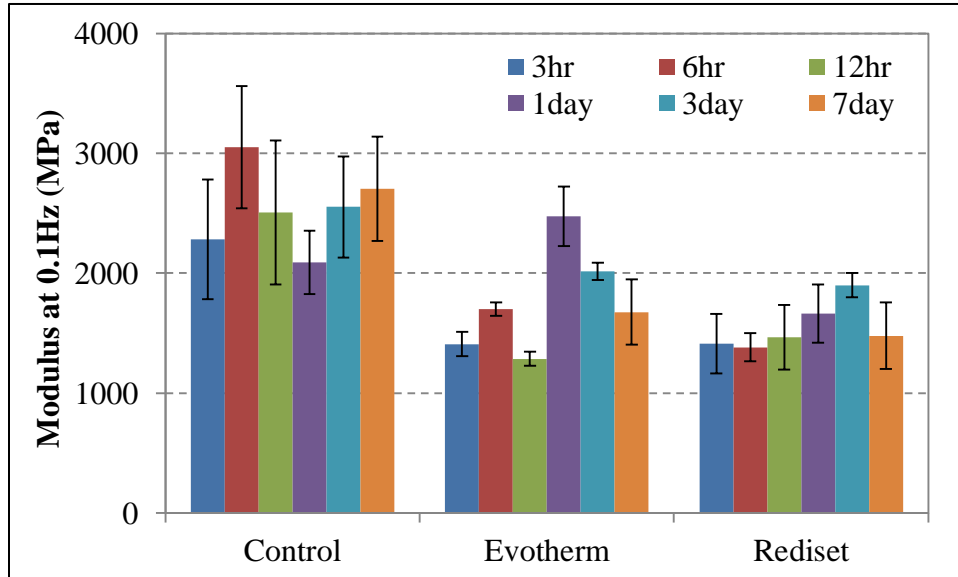

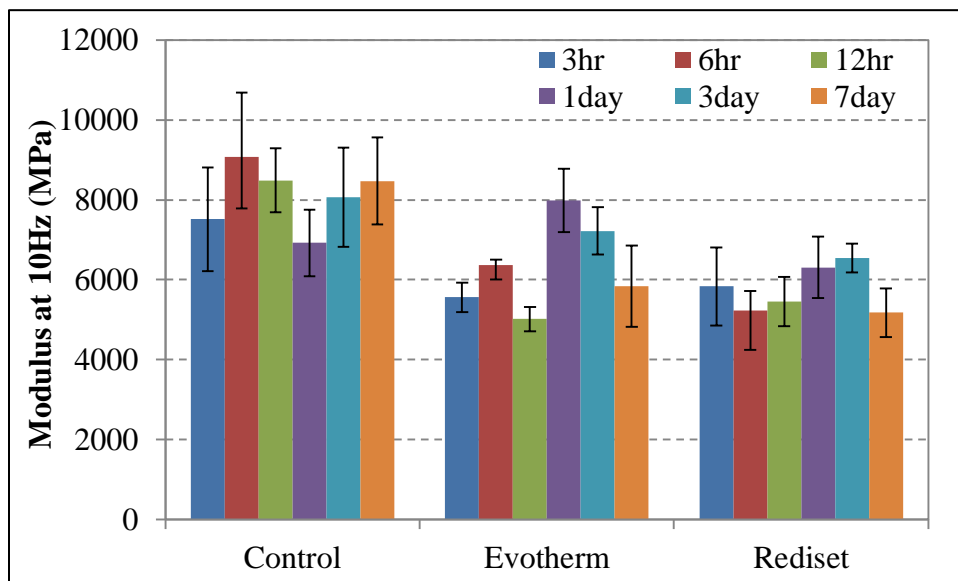**Figure 5.1. Dynamic moduli at 0.1 Hz.**

Figure 5.2. Dynamic moduli at 10 Hz.

Figures 5.1 and 5.2 demonstrate the change of the measured dynamic modulus with varying curing times, comparing the control SMA to the warm-SMAs with Evotherm[TM] 3G and Rediset® at frequencies, 0.1 Hz and 10 Hz, respectively. The following columns indicate average values from three test replicates and the error bars indicate data variability over one standard deviation.

The control SMA exhibited an overall higher dynamic modulus than the two warm-SMAs. In addition, the control SMA and SMA with Rediset® moduli remained relatively constant over various curing periods from a statistical point of view. On the other hand, the SMA with Evotherm[TM] 3G illustrated a sudden modulus increase after one day of curing and gradually decreased throughout the first seven days of curing. The dynamic modulus gain could be attributed to the chemical compositions of Evotherm[TM] 3G. In general, no trend between the dynamic moduli and the curing times could be identified.

5.1.3 Permanent Deformation

Due to the decreased mixing and compaction temperatures of the warm-SMAs, less aging (stiffening) may occur during these stages which can lead to the possibility of rutting or permanent deformation. Therefore, it became essential to investigate the rutting potential of the mixtures.
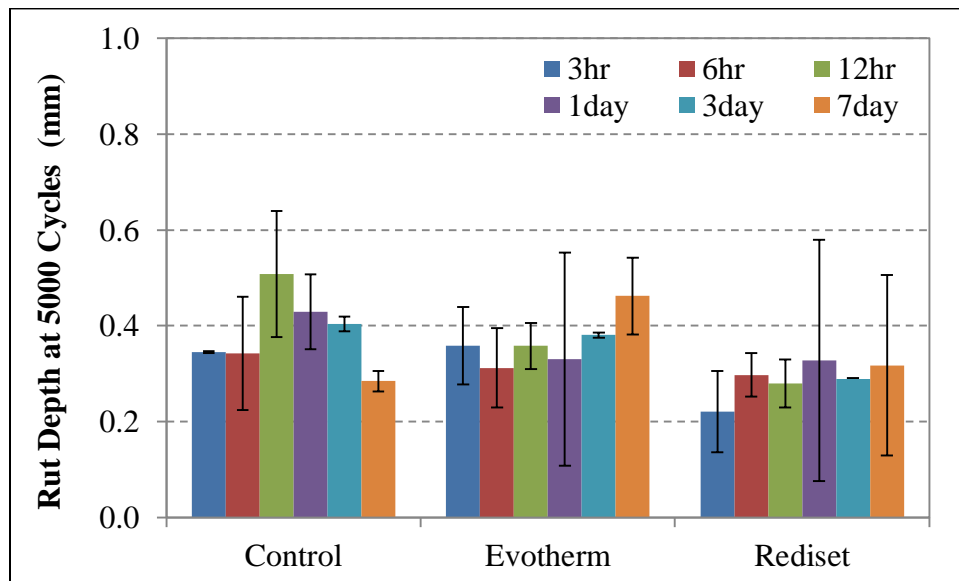

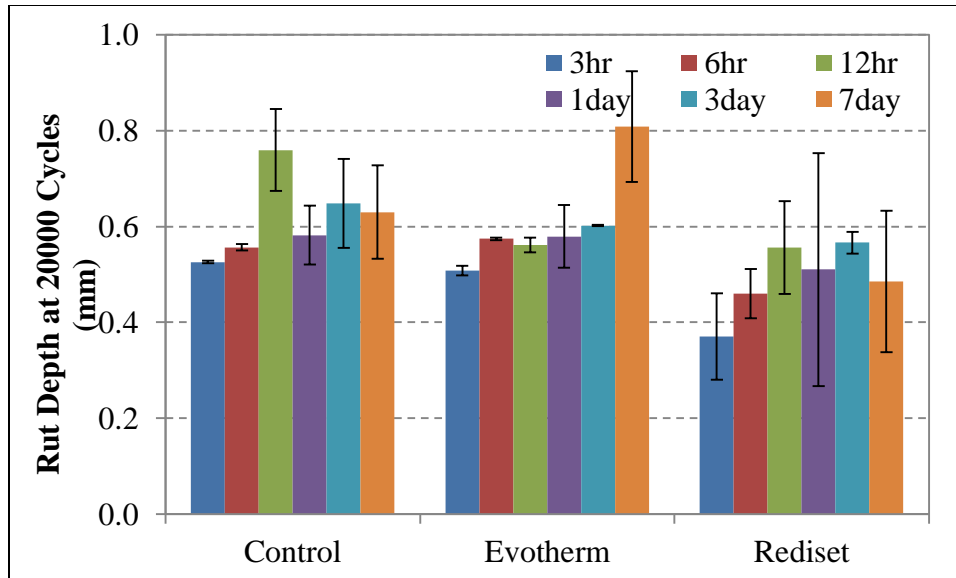**Figure 5.3. Rut depth under dry condition at 5,000 cycles.**

Figure 5.4. Rut depth under dry condition at 20,000 cycles.

Figures 5.3 and 5.4 compare the measured rut depths under dry condition at 30 °C (86 °F) for the control SMA and the two warm-SMAs, which were evaluated at 5,000 and 20,000 cycles in the loaded wheel track tests.

Since the research study focus was the short-term material characterization, it was chosen to perform the loaded-wheel track test under dry conditions at 30 °C (86 °F) and exacerbate it under high temperature. In contrast to expected results, the two warm-SMAs did not show greater rut depths than the control SMA. As illustrated in Figures 5.3 and 5.4, the rut depths of the three mixtures remained relatively constant in the range of 0.3 to 0.5 mm at 5,000 loading cycles.

Furthermore, after the seven day curing period, the SMA with Rediset® resulted in the smallest average rut depth at 20,000 loading cycles, which is the standard threshold used in the State of Illinois for a PG 76-22 asphalt binder for maximum rut depth. The rut depth of the control SMA increased during the first three curing periods, namely three, six and 12 hrs, and decreased to a relatively constant range throughout the last three curing periods, including one, three and seven days. Another observation indicated an increase in the rut depth of the SMA with Evotherm[TM] 3G that was cured for seven days. This behavior may be attributed to the chemical composition of the WMA additive. Nevertheless, the rut depth range of 0.5 to 0.8 mm after 20,000 loading cycles deemed to be statistically insignificant throughout the varied curing period.

Therefore, based on the results it can be concluded that the introduction of the WMA chemical additives to the SMA does not significantly affect the permanent deformation susceptibility of the mixture, despite the increase of the rut depth of the SMA with Evotherm^{TM} 3G at a curing period of seven days. It could also be observed that the SMA with Rediset® resulted in the lowest rut depth throughout the curing period in comparison to the control SMA and SMA with Evotherm^{TM} 3G. It is worth noting that one major factor to the permanent deformation resistance is the highly stable aggregate-to-aggregate interlock of the SMA skeleton.
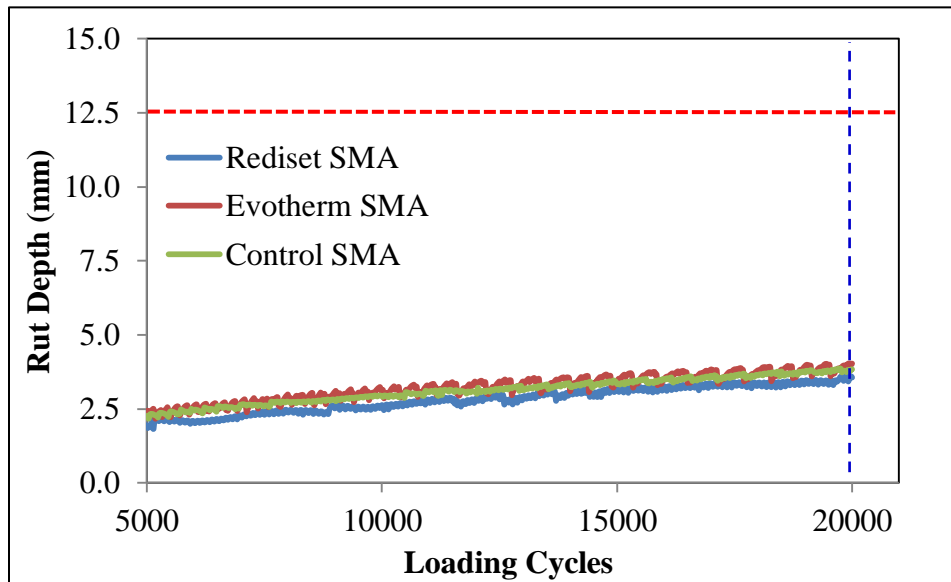
Figure 5.5. Rut depth under wet condition.

However, in order to determine mixture compliance with regards to the loaded-wheel track test specification, the mixtures were also evaluated under the wet condition at 50 °C (122 °F). Figure 5.5 illustrates the rut depths of the three mixtures after seven days of curing in accordance with the loaded-wheel track rutting specification test. The results indicated that the rutting potentials of the three mixtures were relatively the same. Similar to the dry condition results, the SMA with Rediset® provided the lowest rut depth among the three mixtures. In the State of Illinois, the maximum allowable rut depth at 20,000 loading cycles is 12.5 mm (0.5 in). Therefore, based on the loaded wheel track results, it is evident that all three mixtures were in compliance with the specifications, considering that the actual performance grade for the binders with GTR used in these mixtures was PG76-22.

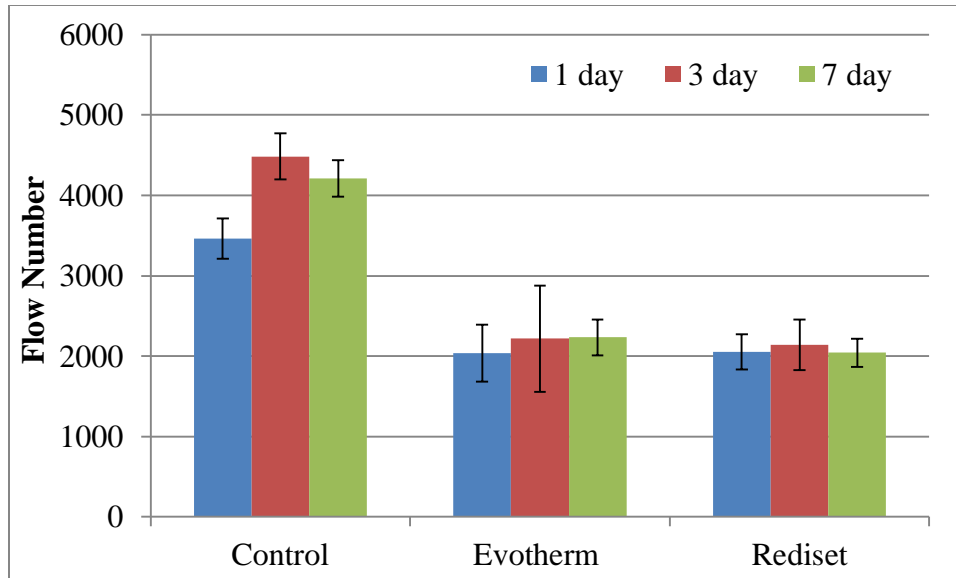**Figure 5.6. Flow number test results.**

The rutting potential of the SMA was also evaluated using the flow number test. However, the flow number test was conducted solely on the mixtures after the 12 hr curing period due to the long test duration. Specimens that were cured under 12 hrs would not be appropriately tested because the test duration is longer than the curing period.

Figure 5.6 indicates the flow number test results at 58 °C (136 °F) for the three SMA mixtures. As aforementioned in the previous chapter, the flow number indicates the point where tertiary flow or permanent deformation occurs. The results demonstrate that as the curing period increases, the flow number remains relatively constant for the warm-SMAs with Evotherm[TM] 3G and Rediset®, whereas the flow number increases after one day curing period and remains relatively constant for the control SMA. In contrary to the loaded-wheel track test qualitative results, the control SMA provides greater rutting resistance in comparison to the warm-SMAs with Evotherm[TM] 3G and Rediset® according to the flow number test results. It has to be noted that both the dry and wet test conditions are not measuring the same characteristics and the loading mechanism of wheel track and flow number tests are different. The wheel track test applies shear loading (along with compression), while the flow number test applies unconfined compression loading.

5.1.4 Indirect Tension

The maximum load for all the specimens with varied curing periods was recorded to calculate the tensile strengths of the three mixtures at room temperature. Figure 5.7 shows the comparison of indirect tensile strengths of the control SMA and the two warm-SMAs at different curing periods. The results exhibit that the two warm-SMAs exhibited lower tensile strengths than the control mixture within the first 12 hrs of curing time after compaction. It is worth noting that the tensile strength of the control SMA remained relatively constant. On the other hand, the SMA with Evotherm^{TM} 3G remained constant within three days of curing, and rapidly increased at seven days of curing; whereas the SMA with Rediset® revealed an increase in the tensile strength as the curing period increased up to one day, decreased during the three-day curing period and increased again on the seventh day of curing. Although the three mixtures presented different trends of tensile strengths throughout the seven day curing period, it is noteworthy that after the seven day curing period, the tensile strengths of the three SMAs reached relatively close ranged values.
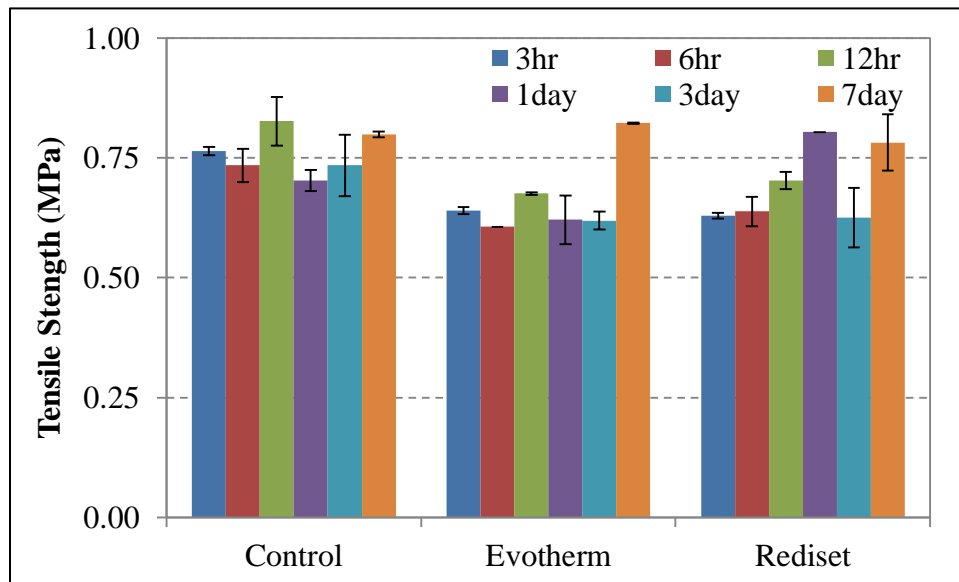

Figure 5.7. Indirect tensile strength results.

5.1.5 Fracture Property

Figure 5.8 compares the fracture energies of the control SMA and two warm-SMAs. The three mixtures demonstrated varied relationship patterns between the fracture energy and curing

time. The fracture energy of the control SMA remained almost constant over the curing period, whereas the fracture energies of the two warm-SMAs gradually decreased after seven days of curing and remained in a relative constant range. Additionally, it can be realized that although the two warm-SMAs had higher fracture energies than the control SMA throughout the seven days of curing period, the fracture energies of the two warm-SMAs seem to be relatively comparable to the nearly constant fracture energy of the control SMA after the first seven days. In general, the fracture energies of the control and warm-SMAs are acceptable.
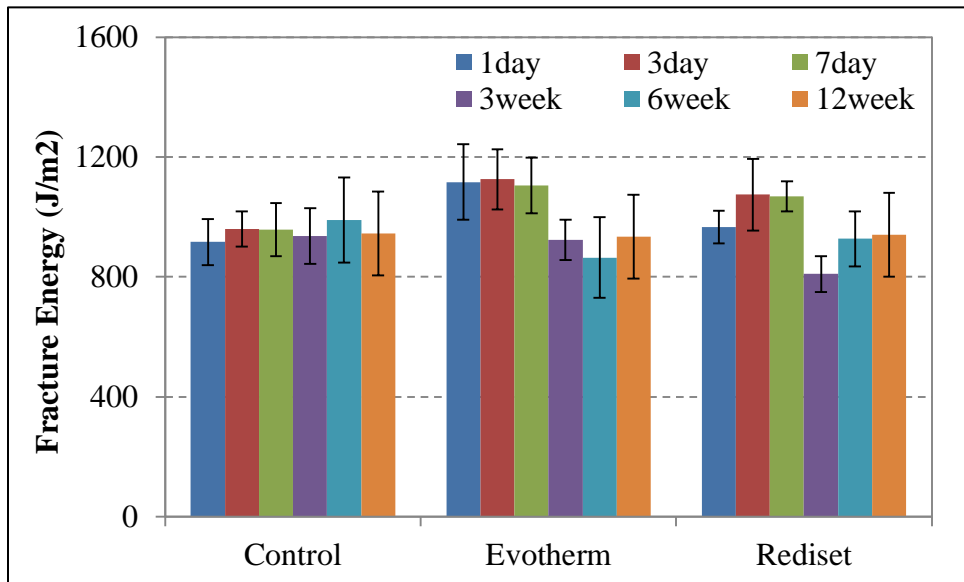
Figure 5.8. SCB fracture energy.

5.2 Statistical Analysis

In order to evaluate repeatability and precision of the results, a statistical analysis is performed using the Statistical Analysis System (SAS) program. Using the analysis of variance (ANOVA), the total sum of squares of the deviations of the observations about the average values are grouped into portions associated with independent variable in the experiment and into a portion associated with the error. There are two components in ANOVA, namely (1) factor, which refers to a categorical quantity under examination in an experiment as a possible cause of variation in the response variable; and (2) level, which refers to the categories, measurements, or strata of a factor of interest in the experiment. A two-way ANOVA was used as it tests the equality of two or more population means when several independent variables or factors are used. Several assumptions using this type of statistical analysis include: normal distribution of

the population, homogeneity of the variance and independence of errors. With this research study, the mixture property was considered as the response variable, while the independent variables included the curing time and mixture type.

Additionally, the Fisher Least Significant Difference (LSD) test was performed alongside the two-way ANOVA in order to consider multiple comparisons of each factor at a significant level of 0.05 *(46)*. The statistical significance of the changes in the mixture properties as a function of curing time and mixture type was evaluated. The test results were ranked using letters, and the letter was changed when the mean was statistically different from others. Letter A was assigned to the highest rating property, followed by other letters in alphabetic order. Using double letter ranking (e.g. A/B) indicated that the difference in the means was not statistically significant and the results could fall in either group.

5.2.1 Curing Period Effect

Tables 5.2 and 5.3 show the Fisher LSD results regarding the effect of curing time on each mixture property for the two warm-SMAs with Evotherm^{TM} 3G and Rediset®, respectively. The complex modulus at 10 Hz and the rut depth in the dry-conditioned load wheel test at 20,000 cycles were used in the statistical analysis.

Table 5.2. Fisher LSD Test Results for the Effect of Curing Time (Evotherm^{TM} 3G SMA).

Mixture Property	Curing time					
	3 hrs	6 hrs	12 hrs	1 day	3 day	7 day
Dynamic Modulus	B/C	B	C	A	A/B	B/C
Rut Resistance	A	A/B	A	A/B	A	B
Tensile Strength	B/C	C	B	C	C	A
Mixture Property	Curing time					
	1day	3day	1week	3week	6week	12week
Fracture Resistance	A	A	A	A/B	B	A/B

Table 5.3. Fisher LSD Test Results for the Effect of Curing Time (Rediset® SMA).

Mixture Property	Curing time					
	3 hrs	6 hrs	12 hrs	1 day	3 day	7 day
Dynamic Modulus	A	A	A	A	A	A
Rut Resistance	A	A	A	A	A	A
Tensile Strength	B/C	B/C	A/B	A	C	A/B
Mixture Property	Curing time					
	1day	3day	1week	3week	6week	12week
Fracture Resistance	A/B	A	A	B	A/B	A/B

From Table 5.2, the following findings can be observed for the SMA with Evotherm^{TM} 3G:

- The dynamic modulus of the SMA with Evotherm^{TM} 3G varied with the curing time. Initially, the dynamic modulus increased after one day of curing time and then decreased after three days. Therefore, a trend with regards to the dynamic moduli cannot be concluded.

- The rutting potential of the SMA with Evotherm^{TM} 3G remained relatively constant within the first seven days, indicating that at the lowest curing period of three hrs will perform similarly to the mixture if cured for seven days.

- The tensile strength of the SMA with Evotherm^{TM} 3G kept relatively constant within the first three days; however increased at seven days.

- The fracture resistance of the SMA with Evotherm^{TM} 3G maintained a constant range for the first seven day curing period, which insinuates that at the lowest curing period of three hrs it will perform relatively the same as the mixture if cured for seven days.

On the other hand, as shown in Table 5.3, the following findings can be observed for the SMA with Rediset®:

- The dynamic modulus of the SMA with Rediset® stayed constant throughout the varied curing period, thereby providing the least significant effect of the curing period from three hrs to seven days.

- The rutting potential of the SMA with Rediset® remained relatively constant throughout the seven day curing period, which determines that the mixture will perform relatively similar throughout the seven day curing period.

- The tensile strength of the SMA with Rediset® varied with curing time. It kept relatively constant throughout one day of curing period then decreased after three days, and increased again at seven days, by which a clear trend cannot be evaluated.

- The fracture resistance of the SMA with Rediset® remained relatively constant throughout the varied curing period, indicating that at the lowest curing period of three hrs will perform similarly to the mixture if cured until seven days.

- In general, the SMA with Rediset® demonstrated stable behavior during the short-term performance tests.

5.2.2 Performance Comparison between Mixtures

The mechanical characteristics of the three SMAs were also statistically evaluated using the two-way ANOVA and Fisher LSD. As shown in Table 5.4, the ranking of mixture performance for each property were grouped together for all curing times to compare the statistical significance of the control SMA to the two warm-SMAs. Similar to the previous section, the dynamic modulus at 10 Hz was used to describe the modulus property of each mixture. However, the rut depth in the wet-conditioned wheel test at 20,000 cycles and the flow number test were used to describe the rut resistance of each mixture.

Table 5.4. Fisher LSD Test Results for the Effect of Mixture Type.

Mixture Property		SMA Mixture		
		Control	Evotherm^{TM} 3G	Rediset®
Dynamic Modulus		A	B	B
Rut Resistance	Loaded Wheel Track (Wet)	A	A	A
	Flow Number	A	A/B	B
Tensile Strength		A	B	B
Fracture Resistance		A	A	A

The following findings can be obtained from the results shown in Table 5.4:

- The control SMA provided a greater dynamic modulus and tensile strength in comparison to the warm-SMAs with Evotherm^{TM} 3G and Rediset®, which may be attributed to less aging that occurs at lower mixing and compaction temperatures for the warm-SMAs.

- The loaded wheel-track test results indicated that the rutting resistance of the control SMA was statistically similar to the two warm-SMAs; whereas according to the flow number test results, the control SMA provided greater rutting resistance than the two warm-SMAs. The different findings from the two rutting performance tests could be attributed to the different specimen setups and loading mechanisms of the loaded wheel-track and flow number tests. In the loaded wheel-track qualitative test, the testing specimens were confined within the molds and were subjected to both shear and compression loadings under the steel wheels. On the other hand, the flow number test was performed without any confinement under compression, therefore only applying compressive loading onto the specimen.

- The tensile strength of the control SMA, as expected, appeared to be statistically higher than the warm-SMAs, which can be attributed to a slightly higher oxidation of the control SMA in comparison to the warm-SMAs due to the increased production temperatures.

- The fracture potential of the three mixtures was statistically the same, thereby indicating that the control and warm-SMAs will perform relatively similar with regards to low-temperature susceptibility.

- Both warm-SMAs indicated no statistical difference with regards to the dynamic modulus, rutting potential, tensile strength, and fracture potential.

The evaluation of short-term mechanical properties of the three mixtures serves as an indicator to field performance. However, solely investigating material properties does not provide a robust comparative analysis of the asphalt concrete mixtures. The next section discusses the economic and environmental impact of the SMAs.

CHAPTER 6.   LIFE CYCLE ASSESSMENT AND LIFE CYCLE COST ANALYSIS

The increase in environmental and economic awareness in recent years has pushed the scientific envelope to develop technologies to reduce hazardous emissions and energy consumptions that resulted from asphalt concrete production and placement. In addition to the material's ability to withstand traffic and environmental loadings, it must meet economic and environmental requirements. For instance WMA, in comparison to conventional HMA, has been found to decrease energy consumption, lower environmental impact, and extend construction seasons. Therefore, in order to provide a realistic and robust evaluation of the material life cycle, both the environmental and economic impact from 'cradle-to-grave', namely from resource extraction through manufacturing, transportation, construction and final disposal, need to be appended to material characterization. Two commonly used tools in the engineering industry to determine these important factors are the life cycle cost analysis (LCCA) and life cycle assessment (LCA).

Life cycle cost analysis is an engineering economic analysis tool that quantifies differential costs of various alternative options for a project. This enables transportation officials to evaluate the specified options and optimize economic benefits. Not only does LCCA consider initial or capital investment, but it also determines all agency and user expenditures. Agency costs, typically include, preliminary engineering, contract administration, construction, maintenance, rehabilitation and all other costs incurred directly by the agency over the project life. On the other hand, user costs are the expenditures incurred by the motoring public due to vehicle operation, traffic delay and accidents.

To append the economic impact investigation, LCA is a tool that quantifies and collates key environmental burdens related to energy use and emissions to air, land and water. Using the LCA indicates the transfer of environmental impacts from one media to another or from one life cycle stage to another. Moreover, it is a tool that can assist in identifying significant environmental shifts between the material's life stages and assess human and ecological effect of material consumption and environmental releases to the neighboring communities.

Therefore, with the combination of LCCA, LCA and mechanistic characterization, transportation officials are better equipped to make a well-informed decision to benefit the users, and optimize the economic and environmental advantages of WMA use.

6.1 Life Cycle Cost Analysis

The economic impact analysis weighs highly on the transportation officials' decision regarding the approval or denial of a given project. The Federal Highway Administration (FHWA) LCCA software, RealCost, was used to evaluate the economic impact of using conventional SMA and warm-SMAs. RealCost evaluates the life cycle values for both the agency and user costs that are associated with the construction and rehabilitation phases of the project. It also enables the comparison of the alternatives in a deterministic sensitivity and probabilistic risk approach. Moreover, the software enables work zone user cost calculation which relates to the realistic traffic demand to roadway capacity during construction.

The LCCA was performed on the control SMA, warm-SMA without RAP and warm-SMA with RAP to investigate the effect of combining the WMA additive and RAP. This combination could reduce energy use and enable cost savings. In order to directly compare the effect of WMA and RAP, the following parameters were considered:

- traffic data, based on the 2011 Illinois Highway Information System (IHIS) database for I-355 at Dupage County;
- hourly traffic distribution;
- added vehicle time and cost;
- construction machinery; and
- construction work time frame.

According to the 2011 IHIS data, the AADT was approximately 62,800 northbound and 63,700 southbound. In addition, the assumed activity service was limited to ten years. More details on the analysis inputs can be found in Appendix A.

6.1.1 Agency Costs

Agency costs are attributed to the construction, maintenance and rehabilitation aspects of a project. In this study, the construction costs differ due to the one lane-mile material costs,

however, the maintenance and rehabilitation costs were equated. Based on the WMA additive manufacturer, the cost of the chemical additive for one ton of warm-SMA is estimated to be $2.50. The fuel consumption savings due to lowering the mixing and compaction temperatures for the warm-SMAs are also considered in the analysis. According to previously collected data, a 15.9% energy reduction in the natural gas usage is enabled by the warm-SMA *(5)*. ISHTA provided that the SMA binder course ranges from $72.00 to $81.00 at the present 2012 cost. The RAP savings, of approximately using 10%, can save about $4.35 for one ton of asphalt mixture in 2007, therefore using the Consumer Price Index, the present 2012 savings corresponded to $6.71. The comparison of the material cost and savings of the control and warm-SMAs are presented in Table 6.1.

Table 6.1. Material cost and savings of mixture.

Mixture	Cost of One Ton of Mixture					Cost of One Lane-Mile of Mixture (685.3 ton)
	SMA	WMA Additive	Fuel Saving	RAP Saving	Total	
Control SMA	$77.0	$0.00	$0.00	$0.00	$77.00	$52,768.10
Warm SMA	$77.0	$2.50	-$0.40	$0.00	$79.10	$54,208.94
Warm SMA with RAP	$77.0	$2.50	-$0.40	-$6.71	$72.40	$49,613.15

Additionally, the construction cost of the SMA, including production and placement costs, was $25.00 per ton. Therefore, the total cost of three mixtures per lane-mile is shown in the following table (Table 6.2).

Table 6.2. Total cost of mixture.

Mixture	Cost of One Lane-Mile of Mixture (685.3 ton)
Control SMA	$69,900.60
Warm SMA	$71,341.44
Warm SMA with RAP	$66,745.65

6.1.2 User Costs

User costs are estimated based on the delay of travel that is caused by the pavement construction. Seven components are considered in the user cost calculation. In regards to the free-flow state, the first three components include speed change delay, speed change vehicle operation cost (VOC), and reduced speed delay. In addition, the remaining four components which correspond to the forced flow state include stopping delay, stopping VOC, queue delay and idle VOC.

A triangular distribution was used for the discount rate, by which 3% was the minimum, 4% was depicted to be the most likely value, and 5% was the maximum. The free flow capacity was then calculated using the RealCost software based on the traffic data provided. Based on previous studies, the queue dissipation capacity was modeled as a normal distribution with 1818 vehicles per hour per lane (vphpl) as the average value and a standard deviation of 144 *(47)*. Accordingly, the user time values were updated from 1996 dollar values (estimated by the FHWA) onto the 2012 dollar values using the Consumer Price Index (CPI) according to the Bureau of Labor Statistics *(47)*. The CPI escalation value from 1996 to 2012 was calculated to be 1.4758. Similar to the discount rate, a triangular distribution was utilized for the user time values as well (Table 6.3). The speed limit was reduced from a normal speed of 55 mph (89 km/hr) to the work zone speed of 45 mph (72 km/hr). Lastly, the work zone capacity was estimated to be 1,340 vphpl according to *(47)*.

Table 6.3. Values of User Time Escalated from Year 1996 to 2012.

Values of User Time ($/hr)	Year 1996			Year 2012		
Vehicle Class	Min ($)	Most Likely ($)	Max ($)	Min ($)	Most Likely ($)	Max ($)
Passenger	$10.00	$11.58	$13.00	$16.29	$18.86	$21.18
Single-unit	$17.00	$18.54	$20.00	$27.69	$30.20	$32.58
Combination Trucks	$21.00	$22.31	$24.00	$34.21	$36.35	$39.10

6.1.3 Deterministic Results

The control SMA was compared to the warm-SMA and warm-SMA with RAP in order to determine the effect of WMA additive and RAP on the cost of SMA. It is worth noting that the

work zone hours are optimized to a night paving scenario from 9 PM to 5 AM, wherein user costs are reduced significantly in contrast to the paving operations during the day. Table 6.4 shows the present total cost of the SMAs per lane-mile based on the deterministic analysis.

Table 6.4. Total cost of mixture per lane-mile based on LCCA deterministic results.

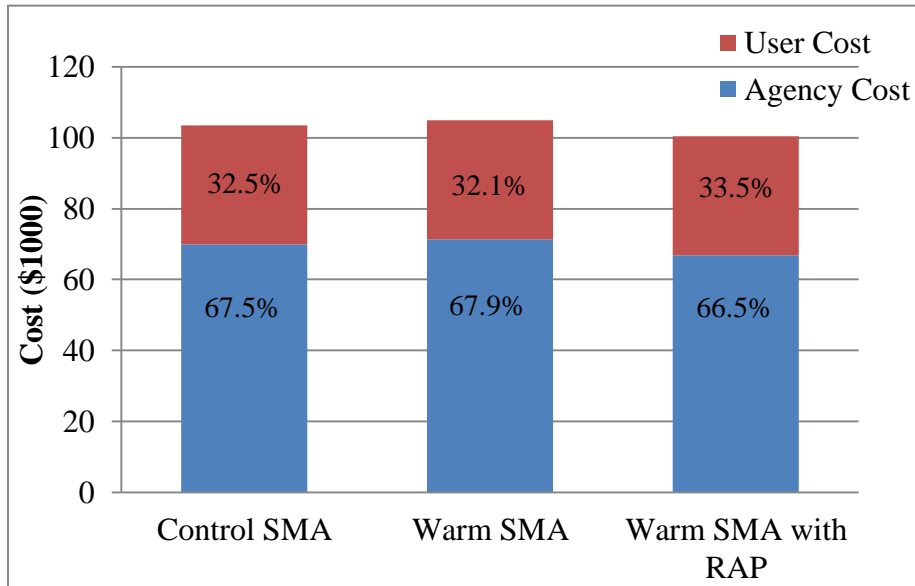| Present Cost ($1000)	Mixture		
	Control SMA	Warm SMA	Warm SMA with RAP
Agency Cost	$69.90	$71.34	$66.75
User Cost	$33.66	$33.66	$33.66
Total	$103.56	$105.00	$100.41

Figure 6.1. Deterministic LCCA results.

Using the deterministic sensitivity analysis, economic impacts of the control SMA, warm-SMA and warm-SMA with RAP were compared. Based on the results, a 3% reduction in the total cost of the warm-SMA with RAP was determined in comparison to the control SMA. Additionally, it can be observed that the warm-SMA with RAP resulted in the lowest present agency cost, while the warm-SMA resulted in the lowest present user cost (Figure 6.1).

6.1.4 Probabilistic Results

The probabilistic analysis was performed in order to quantify the risk and uncertainty of various variables. Inputs used in the analysis are dependent upon several factors and assumptions, which may lead to uncertain variables. The conditions used for the probabilistic analysis include a maximum of 2,000 iterations with a convergence tolerance of 2.5%. The final probabilistic simulation of the given conditions converged to 2,000 iterations with a final error of 3.37%.

Table 6.5. Probabilistic LCCA results.

Total Cost	Total Cost					
	Control SMA		Warm SMA		Warm SMA with RAP	
Total Cost	Agency Cost ($1000)	User Cost ($1000)	Agency Cost ($1000)	User Cost ($1000)	Agency Cost ($1000)	User Cost ($1000)
Mean	$69.90	$33.70	$71.34	$33.70	$66.75	$33.70
Standard Deviation	$0.00	$1.44	$0.00	$1.44	$0.00	$1.44
Minimum	$69.90	$30.12	$71.34	$30.12	$66.75	$30.12
Maximum	$69.90	$37.08	$71.34	$37.08	$66.75	$37.08

It is noted that, the user cost had relatively a higher impact on the uncertainty in comparison to the agency cost. It is noteworthy that the tabulated results do not include specific construction machineries and processes for each mixture. Because the user cost is mainly affected by the construction period, the user cost for each mixture remained the same (Table 6.5). This is due to the fact that the optimized construction period for all the mixtures was set to the same night paving period.

6.2 Life Cycle Assessment

In order to quantify the environmental impact of the three SMAs, a 'cradle-to-grave' life cycle assessment was conducted. Two phases that contribute mostly to the energy consumption are raw material acquisition and mixture production. There are four major steps in the LCA framework (Figure 6.2);
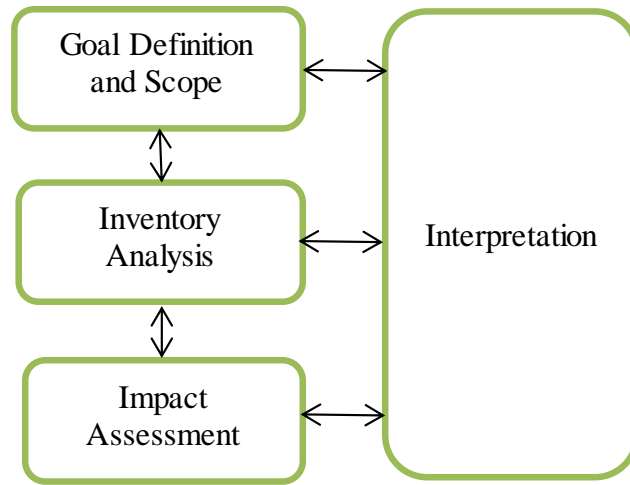
Figure 6.2. Basic LCA framework.

(1) goal and scope definition, wherein the system boundaries are established and the functional unit is defined;

(2) inventory analysis, indicating the consumption of resources and quantities of waste and emission from the selected system boundaries;

(3) impact assessment; and

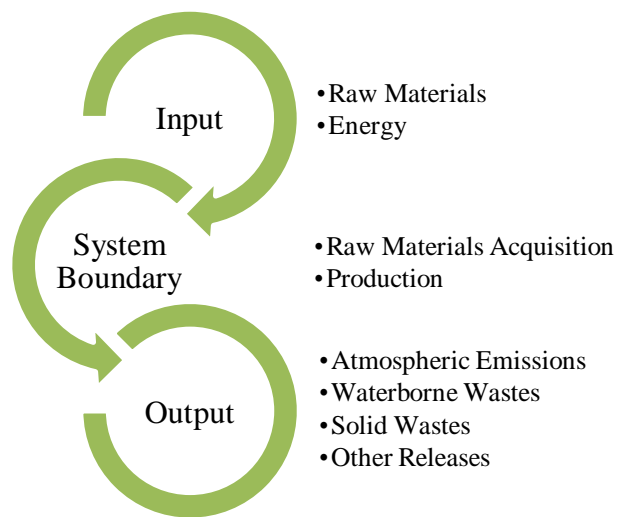(4) life-cycle interpretation, by which performance scores on the environment and economic impacts are justified.

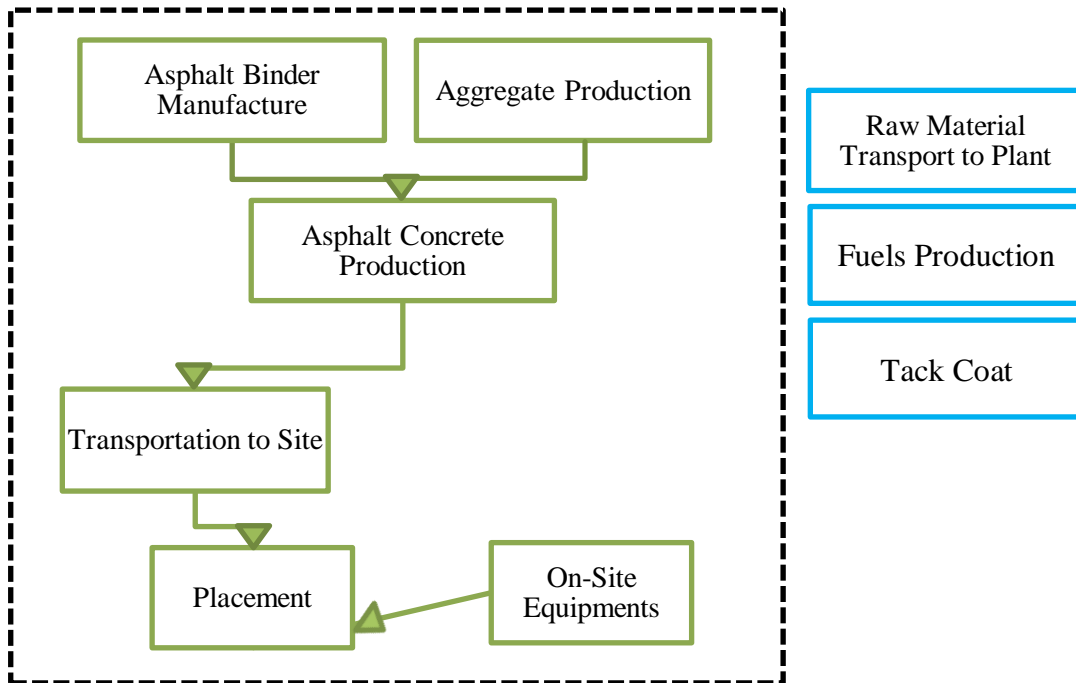**Figure 6.3. Life cycle assessment stages.**

Figure 6.4. LCA system boundary.

The 'cradle-to-grave' LCA stages are presented in Figure 6.3, which considers the typical input and output parameters measured. The system boundary of the LCA study included raw material acquisition, plant production, mixture transport and construction (Figure 6.4). In addition, by compiling an inventory of relevant energy and material inputs and environmental releases, the potential environmental impacts can be used by decision-makers to make a more informed decision. Table 6.6 presents the life cycle inventory for a one lane-mile of control SMA, containing 6.2% asphalt binder (42.5 ton [38.5 metric ton]) and 93.8% crushed aggregates (642.8 ton [583.1 metric ton]), which pertains to the mixture design. The assumed transportation distance from the asphalt concrete plant to the construction site was 19 miles (36 km) and the paving speed was 160 ton/hr (145.1 metric ton/hr).

Table 6.6. Life cycle inventory for one-lane mile of control SMA.

Production of 1 ton SMA (process with infrastructure)	Asphalt (ton)	Aggregate (ton)	Production (ton)	Transport (ton-mile)	Paving (hr)	Breakdown Rolling (hr)	Finish Rolling (hr)
	42.5	642.8	685.3	13020.7	4.3	4.3	4.3
Consumption of energy resource	(BTU)						
Natural gas	1.47E+07	1.09E+05	6.30E+07	-	-	-	-
Oil	3.54E+06	1.11E+07	2.18E+08	-	-	-	-
Electricity	3.17E+05	5.50E+06	4.18E+07	-	-	-	-
Fuel	-	-	-	1.53E+07	8.78E+06	8.78E+06	3.25E+06
Emissions	(g)						
CO2	8.71E+06	8.28E+05	2.03E+10	6.74E+04	2.99E+05	2.94E+05	1.27E+05
SOx	3.46E+04	4.59E+02	3.06E+07	3.24E+01	2.99E+01	2.93E+01	1.27E+01
NOx	4.40E+04	7.17E+03	7.01E+07	4.30E+02	2.42E+03	2.43E+03	1.08E+03
CO	4.00E+04	8.66E+02	6.95E+06	6.83E+01	7.54E+02	7.67E+02	8.70E+02
CH4	2.76E+04	2.23E+00	6.30E+03	4.27E-02		-	-
VOC	1.56E+04	5.19E+02	7.60E+06	9.47E+02	1.83E+02	1.84E+02	1.19E+02
Particulates	1.16E+04	1.14E+03	2.23E+06	7.22E+00	2.94E+02	2.96E+02	2.48E+02

Conversion: 1 ton = 0.91 metric ton; 1 BTU = 1.06 kJ; 1 g = 0.002 lb

Various energy and emission databases were used to discretize and create the life cycle inventory of the control SMA *(48-53)*. Based on previous studies, it was determined that by reducing the mixing temperature from 180 to 125 ^{o}C (356 to 257 ^{o}F), the energy consumption can be reduced by 35% due to the use of WMA *(2, 54)*. It was assumed that the reductions of energy consumption were correlated proportionally to the temperature reduction. In this study, the mixing temperature was reduced from 163 to 138 ^{o}C (325 to 280 ^{o}F). Table 6.7 indicates emission reductions, which were incorporated into the life cycle inventory to compare the environmental impact of the control and warm SMAs.

Table 6.7. Emission reduction proportional to temperature reduction.

Emission	Emission Reduction (356 ^{o}F to 257 ^{o}F)	Emission Reduction (325 ^{o}F to 280 ^{o}F)
CO2	25.0%	11.4%
SOx	60.0%	27.3%
NOx	35.0%	15.9%
CO	8.0%	3.6%
Particulate	28.0%	12.5%

Conversion: ^{o}C = (5/9) (^{o}F - 32)

In order to fully comprehend the comparison of the environmental impacts of the SMAs, four impact categories were considered, including global warming, fossil fuel depletion, criteria air pollutants, and photochemical smog *(55)*. Previous studies have determined that those are the main impact categories associated with asphalt concrete mixtures *(56)*. Based on the International Standards Organization *(57)*, for each impact category, characterization factors are used to determine the relative impact of the environmental flows. It can be realized that for a large characterization factor, the specified environmental flow has a significantly large impact. Based on the Building for Environmental and Economic Sustainability (BEES) mode, the table below presents the characterization for each impact category *(58, 59)*.

Table 6.8. Characterization factors for each impact category.

Emission Flow	Impact Category			
	Global Warming (CO2-e/g)*	Fossil Fuel (MJ/kg)	Criteria Air Pollutant (micro-DALYs/g)	Photochemical Smog (NOx-e/g)*
Coal	0	0.25	0	0
Oil	0	7.8	0	0
Natural Gas	0	6.12	0	0
CO2	1	0	0	0
SOx	0	0	0	0
NOx	0	0	0.0022	1
CO	0	0	0	0
Particulate	0	0	0.0834	0
VOC	0	0	0	0
CH4	23	0	0	0.003
N2O	296	0	0	0.7806

Global warming potential (GWP) describes the absorption of the sun's radiation, which is redistributed by the atmosphere and ocean and radiated back into space at longer wavelengths, by which some of the thermal radiation may be absorbed by 'greenhouse' gasses in the atmosphere. The radiation of the absorbed energy is eventually lost to space or to colder levels in the atmosphere. However, with the presence of greenhouse gasses, there is less heat surface losses to space, which consequently creates a warmer atmosphere or a 'blanket' around the earth. Global warming potential has been developed in order to characterize the increase of greenhouse gas effect due to humankind emissions. The quantity of carbon dioxide for GWP over a 100-year period can be calculated as follows:

$$global\ warming\ index = \sum_i m_i * GWP_i \tag{6.1}$$

where,

m_i is mass of inventory flow i in g; and

GWP_i is grams of carbon dioxide with the same heat trapping potential over 100 years as one gram of inventory flow i.

Fossil fuel depletion (FFD), on the other hand, determines the level of depletion of the fossil fuel resource and value society places on the depletion, which may be influenced by many factors including resource demand and non-perfect markets. In order to assess this impact category, the amount of energy required to extract a unit of energy is measured for the consumption changes over time. The computation of a single index and assessment of the surplus energy requirement from the consumption of fossil fuels is as follows:

$$fossil\ fuel\ depletion\ index = \sum_i c_i * FP_i \tag{6.2}$$

where,

c_i is consumption of fossil fuel i in kg; and

FP_i is MJ input requirement increase per kilogram of consumption of fossil fuel i.

Moreover, criteria air pollutions (CAP) are solid and liquid particles that are commonly found in the air, arising from a multitude of activities namely, combustion, vehicle operation, power generation, materials handling, and crushing operations. Its functional unit, disability-adjusted life years (DALYs) has been developed in order to quantify health losses from outdoor air pollution, accounting for lost life years, and disability years that are adjusted for the severity of the resulting health conditions. Quantification of this impact category may be obtained using the following equation:

$$criteria\ air\ pollutants\ index = \sum_i m_i * CP_i \tag{6.3}$$

where,

m_i is mass of inventory flow i in g; and

CP_i is microDALYs per gram of inventory flow i.

Lastly, the smog formation potential evaluates industrial and transportation air emissions that can be trapped at ground level, thereby reacting with the sun and resulting to the photochemical smog (PS). Ozone is one of the major components of smog, which is produced through the interactions of volatile organic compounds (VOC) and oxides of nitrogen (NOx). This smog may lead to harmful impacts to human and agricultural health. The characterization factor enables the computation of a single index for potential smog formation:

$$smog\ formation\ potential\ index = \sum_i m_i * SP_i \qquad (6.4)$$

where,

m_i is mass of inventory flow *i* in g; and

SP_i is grams of NOx with the same potential for smog formation as one gram of inventory flow *i*.

In order to reflect the importance of each environmental factor affecting the users, the performance measures are normalized based upon a set of weights as indicated on Table 6.9. Moreover, the relative importance weights for the impact categories are assumed to be 56%, 19%, 17% and 8% for global warming, fossil fuel depletion, criteria air pollutants and smog, respectively *(58)*.

Table 6.9. Normalization values pertaining to each environmental impact.

Impact Category	Normalization Value
Global Warming	25, 582, 640.09 g CO2 equivalent/year/capita
Fossil Fuel Depletion	35, 309.00 MJ surplus energy/year/capita
Criteria Air Pollutants	19, 200.00 microDALYs/year/capita
Smog	151, 500.03 Nox equivalents/year/capita

Figure 6.5 illustrates the comparison of the energy consumption between the control and warm SMAs. It was determined that the main process that influenced the reduction of the energy consumption is the asphalt concrete production, which corresponds to the hypothesis of lowered production temperatures for WMA. Due to the reduced mixing temperature of 163 to 138 $^{\circ}$C (325 to 280 $^{\circ}$F), the energy consumption of the production and other three processes (construction, transport and material) are decreased by 15.9% and 6.5% respectively.
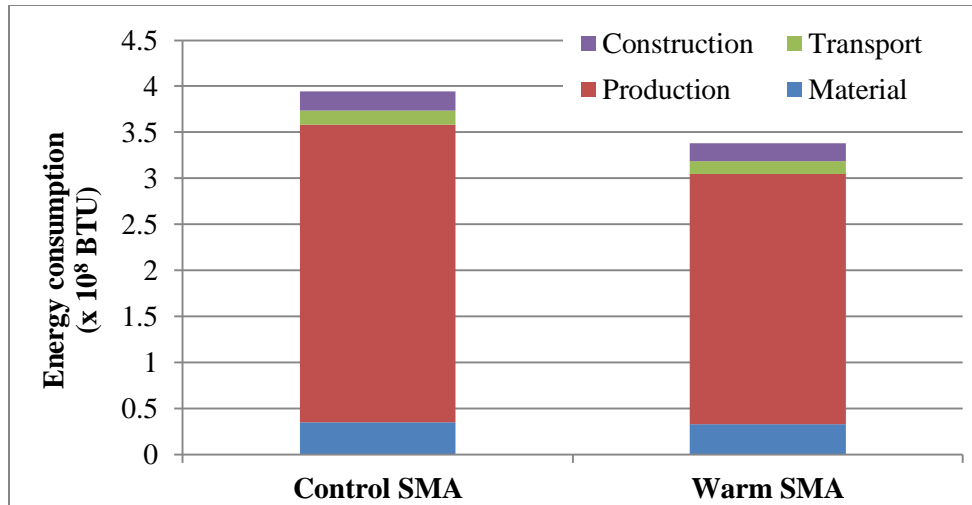
Figure 6.5. Energy consumptions of control and warm SMAs.

Based on the index calculation of the four major impact categories, namely global warming potential, fossil fuel depletion, criteria air pollutant and photochemical smog, the percentage contribution to the overall environmental impact of the control SMA was evaluated (Table 6.10). It could be recognized that the production process had the highest impact on the environment, followed by the material acquisition stage in comparison to the construction and transport phases.

Table 6.10. Contribution to overall environmental impact of control SMA.

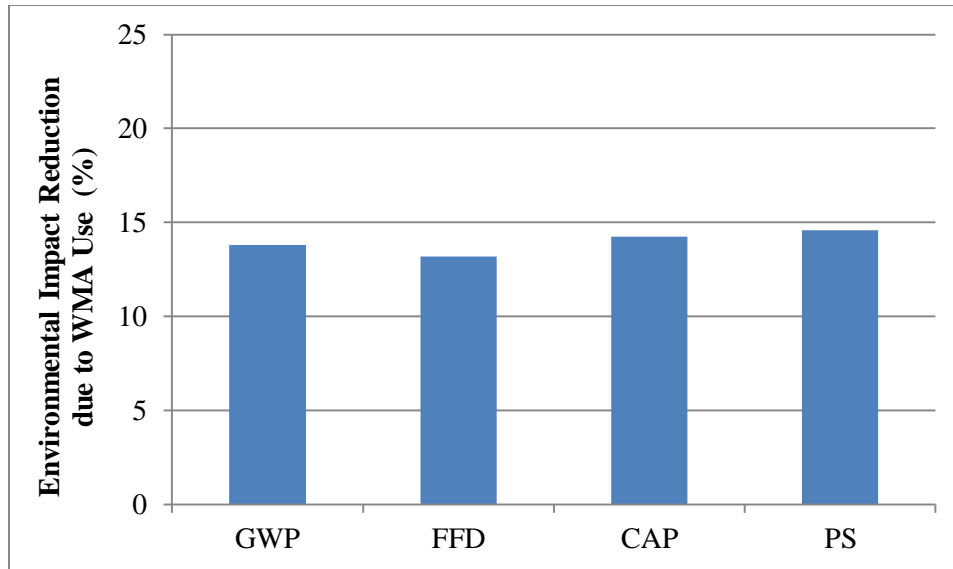| Process	Impact Factor (%)			
	GWP	FFD	CAP	PS
Material	0.06	8.08	0.34	0.07
Production	99.93	82.20	99.63	99.92
Transport	0.00	4.71	0.00	0.00
Construction	0.01	5.02	0.02	0.01

Figure 6.6. Environmental impact reduction due to WMA use.

As illustrated in Figure 6.6, it can be observed that the warm-SMA decreased the global warming potential, fossil fuel depletion, criteria air pollutant and photochemical smog by 13.8%, 13.2%, 14.2% and 14.6%, respectively. Moreover, by using the normalization values presented on Table 6.9, the normalized value of each impact category and a single environmental impact score were calculated for both the control and warm SMAs. It can be observed that the warm-SMA was 13.8% lower than the control SMA, indicating that the warm-SMA is more sustainable and environmentally friendly than the control SMA (Table 6.11).

Table 6.11. Environmental impact score of control and warm SMAs.

Environmental Impact Category	**Control SMA**	**Warm SMA**
Global Warming	8.99	7.76
Fossil Fuel Depletion	0.00	0.00
Criteria Air Pollutants	0.03	0.03
Smog	0.66	0.55
Environmental Impact Score	**9.68**	**8.34**

CHAPTER 7.   SUMMARY, FINDINGS, CONCLUSIONS AND RECOMMENDATIONS

7.1 Summary

The emerging use of WMA technology leads to numerous economic and environmental benefits for transportation agencies and road users. One of the most significant attributes of the WMA technology is its capability to reduce production and laydown temperatures. However, decreased temperatures can pose challenges to adequately obtain the desired mechanical properties to withstand traffic and environmental loading once the pavement is constructed. A performance evaluation addressing different 'curing' periods of the WMA is presented to determine the evolution of the material properties over time and to experimentally characterize the short-term performance of WMA produced with two types of chemical additives, namely Evotherm^{TM} 3G and Rediset® LQ-1106. Based on this study, the following findings and conclusions can be drawn.

7.2 Findings

The study resulted in the following findings on the effect of curing time on the control SMA and warm-SMAs, prepared with Evotherm^{TM} 3G and Rediset® LQ-1106 additives:

- The control SMA exhibited greater dynamic modulus than the two warm-SMAs. However, the effect of curing time on the dynamic modulus is limited and a clear trend between the moduli and the curing time could not be established. For the control SMA and SMA with Evotherm^{TM} 3G, the dynamic modulus increased at the second curing time interval of six hrs, whereas it remained relatively constant for the SMA with Rediset®.

- The inclusion of WMA chemical additives in SMA did not significantly affect the permanent deformation behavior of the mixture when exposed to loading. The SMA with Rediset® resulted in the lowest rut depth throughout the seven-day curing period in comparison to the control SMA and SMA with Evotherm^{TM} 3G.

- As the curing period increased, the flow number remained relatively constant for the two warm-SMAs with Evotherm^{TM} 3G and Rediset®, whereas the flow number increased after a one day curing period and remained relatively constant for the control SMA. The control SMA based on the flow number test, exhibited lower rutting potential in

comparison to the two warm-SMAs. On the other hand, the loaded-wheel track test results revealed similar rut depth for all mixtures at the same number of passes. The results of these two tests, although indicative of the rutting potential, are incomparable due to variations in loading mechanisms and measured response parameters.

- The two warm-SMAs exhibited lower tensile strengths than the control SMA within the first 12 hrs of curing time after compaction. While the tensile strength of the control SMA remained relatively constant, the two warm-SMAs increased during the first seven days. After the seven-day curing period, all SMAs resulted in similar tensile strengths.

- The fracture energy of the control SMA remained almost constant over the curing period, while the fracture energies of the two warm-SMAs gradually decreased after seven days of curing and remained relatively constant after 12 weeks. Although the two warm-SMAs had greater fracture energies than the control SMA throughout the first seven days of curing, the fracture energies of all mixtures became relatively comparable after one week of curing. In general, the fracture energies of the control and warm-SMAs are acceptable and indicated reduced low-temperature cracking susceptibility.

Based on statistical analysis, the following findings can be observed for the SMA with Evotherm^{TM} 3G:

- The dynamic modulus of the SMA with Evotherm^{TM} 3G varied with curing time. Initially, the modulus increased after one day of curing time and then decreased after three days. However, a clear trend could not be established.

- The rutting potential of the SMA with Evotherm^{TM} 3G remained relatively constant over the seven-day measurement period. This suggests that after the first measurements at three hrs of curing, curing time has no effect on the rutting potential.

- The tensile strength of the SMA with Evotherm^{TM} 3G remained relatively constant within the first three days of curing. However, it slightly increased at seven days.

- The fracture potential of the SMA with Evotherm^{TM} 3G maintained within a constant range over the testing period. This suggests that a curing period of three hrs would be sufficient to achieve the desired fracture energy.

On the other hand, the following findings can be observed for the SMA with Rediset®:

- The dynamic modulus of the SMA with Rediset® remained constant throughout the varied curing period. Hence, the curing period after three hrs has minimal effect on the measured dynamic modulus.

- The rutting potential of the SMA with Rediset® remained relatively constant throughout the seven-day curing period.

- The tensile strength of the SMA with Rediset® varied with curing time. It remained relatively constant during the first day of curing period, decreased after three days, and increased again at seven days.

- The fracture potential of the SMA with Rediset® remained relatively constant throughout the seven-day curing period, suggesting minimal effect of curing time on the fracture energy after the first three hrs of curing.

The statistical results of the three SMAs suggest the following findings:

- The control SMA provided a greater dynamic modulus and tensile strength than the two warm-SMAs. This could be attributed to the possible lower mixing and compaction aging of the warm-SMAs, which results in less binder stiffness.

- The loaded-wheel track test results suggested that the control SMA rutting potential was statistically similar to that of the two warm-SMAs. However, the flow number test results indicated that the warm-SMAs could have greater rutting potential compared to the control SMA. The difference in the findings between the two rutting performance tests could be attributed to specimen geometry, loading mechanism, and performance-measured parameter.

- The tensile strength of the control SMA appeared to be statistically greater than that of the warm-SMAs, which could be attributed to the possible greater aging of the control SMA in comparison to the warm-SMAs, which are produced and compacted at relatively lower temperatures.

- The fracture potentials of the three SMAs were statistically the same. Hence, the control and warm SMAs would be expected to perform relatively similar with regards to low-temperature susceptibility.

- The two warm-SMAs results suggested no statistical difference in material measured characteristics including the dynamic modulus, rutting potential, tensile strength, and fracture resistance.

7.3 Conclusions

Based on the results of this study, the following conclusions are made:

1. Based on the mechanical characterization of the control SMA and warm-SMAs with Evotherm^{TM} 3G and Rediset®, the study concluded that, the two warm-SMAs performed relatively similar to the control SMA.
2. No clear trend could be established between the curing periods and the short-term mechanical properties for the control and warm SMAs.
3. The warm-SMA presented more economic and environmental benefits than the control SMA. In addition, incorporating recycled asphalt pavement (RAP) and ground tire rubber (GTR) in warm SMA would only improve such benefits.

7.4 Recommendations for Future Research

- This study presents a short-term mechanical property investigation of warm-SMAs prepared with two chemical additives. It is necessary to advance this evaluation to determine the long-term behavior of the mixtures.
- The reported research study encompassed a specific type of SMA. Extending future studies to include a broad spectrum of mixture types, various percentage contents and types of WMA additives should be considered.
- Moisture susceptibility of warm-SMA should be further investigated.
- The LCCA performed in this research study considered the raw material and construction costs of the asphalt mixtures. Maintenance, end-of-life, rehabilitation and recycling costs should be considered.
- Lastly, limited warm-SMA life cycle inventory has been produced in the United States due to scarce data; therefore, data from Europe was used. Energy and emission databases in the United States should be established to generate a more realistic and current evaluation.

REFERENCES

1. Prowell, B., and G. C. Hurley. Evaluation of Evotherm for use in Warm Mix Asphalt. *NCAT Report 06-02*, June 2006.

2. D'Angelo, J., E. Harm, J. Bartoszek, G. Baumgardner, M. Corrigan, J. Cowsert, T. Harman, M. Jamshidi, W. Jones, D. Newcomb, B. Prowell, R. Sines, and B. Yeaton. Warm Mix Asphalt: European Practice. *FHWA Report no. FHWA-PL-08-007*, February 2008.

3. Brown, E., and H. Manglorkar. Evaluation of Laboratory Properties of SMA Mixgtures. *NCAT, National Asphalt Paving Association Research and Education Foundation.*, 1993.

4. Moghadas Nejad, F., E. Aflaki, and M. A. Mohammadi. Fatigue Behaviour of SMA and HMA Mixtures. *Construction and Building Materials*, Vol. 24(7), 2010, pp. August 10, 2012-1158-1165.

5. Leng, Z., and I. Al-Qadi. Comparative Life Cycle Assessment between Warm SMA and Conventional SMA. *Illinois Center for Transportation Series*, Vol. No. 11-090, September 2011.

6. Prowell, B., G. C. Hurley, and E. Crews. Field Performance of Warm-Mix Asphalt at National Center for Asphalt Technology Test Track. *Transportation Research Record: Journal of the Transportation Research Board*, Vol. No. 1998, 2007, pp. 96-102.

7. Wasiuddin, N. M., S. Selvamohan, M. M. Zaman, and M. L. Guegan. Comparative Laboratory Study of Sasobit and Aspha-Min Additives in Warm-Mix Asphalt. *Transportation Research Record: Journal of the Transportation Research Board*, Vol. No. 1998, 2007, pp. 82-88.

8. Mallick, R. B., P. S. Kandhal, and R. L. Bradbury. Using Warm-Mix Asphalt Technology to Incorporate High Percentage of Reclaimed Asphalt Pavement Material in Asphalt Mixtures. *Transportation Research Record: Journal of the Transportation Research Board*, Vol. No. 2051, 2008, pp. 71-79.

9. Xiao, F., S. N. Amirkhanian, and B. Putnam. Evaluation of Rutting Resistance in Warm-Mix Asphalts Containing Moist Aggregate. *Transportation Research Record: Journal of the Transportation Research Board*, Vol. No. 2180, 2010, pp. 75-84.

10. Hurley, G. C., and B. Prowell. Evaluation of Aspha-Min® Zeolite for use in Warm Mix Asphalt. *Report NCAT 05-04*, 2005a.

11. Hurley, G. C., and B. Prowell. Evaluation of Sasobit® for use in Warm Mix Asphalt. *NCAT Report 05-06*, 2005b.

12. Hurley, G. C., and B. Prowell. Evaluation of Evotherm® for use in Warm Mix Asphalt. *NCAT Report 06-02*, 2006.

13. Prowell, B., and G. C. Hurley. Warm-Mix Asphalt: Best Practices. , Vol. 2nd Edition, 2011.

14. Chowdhury, A., and J. W. Button. A Review of Warm Mix Asphalt. *Report 473700-00080-1*, 2008.

15. Chaffin, J. M., M. Liu, R. R. Davison, C. J. Glover, and J. A. Bullin. Supercritical Fractions as Asphalt Recycling Agents and Preliminatry Aging Studies on Recycled Asphalts. *Ind. Eng. Chem. Res.*, Vol. 36(3), 1997, pp. 656-666.

16. Daniel, J. S., and A. Lachance. Mechanistic and Volumetric Properties of Asphalt Mixtures with Recycled Asphalt Pavement. *Transportation Research Record: Journal of the Transportation Research Board*, Vol. No. 1929, 2005, pp. 28-36.

17. Kandhal, P. S., and K. Y. Foo. Designing Recycled Hot Mix Asphalt Mixtures using Superpave Technology. , 1997, pp. 101-117.

18. Lewandowski, L. H., R. Graham, and J. Shoenberger. Physicochemical and Rheological Properties of Microwave Recycled Asphalt Binders. *Proc., Materials Engineering Congress*, 1992, pp. 449-461.

19. McDaniel, R. S., A. Shah, G. A. Huber, and V. L. Gallivan. Investigation of Properties of Plant-Produced RAP Mixtures. *Transportation Research Record: Journal of the Transportation Research Board*, Vol. No. 1998, 2007, pp. 103-111.

20. Peterson, R. L., H. R. Soleymani, R. M. Anderson, and R. S. McDaniel. Recovery and Testing of RAP Binders from Recycled Asphalt Pavements. *Association of Asphalt Paving Technologies Proc*, No. 69, 2000, pp. 72-91.

21. Terrel, R. L., and D. R. Fritchen. Laboratory Performance of Recycled Asphalt Concrete. *ASTM Special Technical Publication*, 1978, pp. 104-122.

22. Yamada, M. Characterization of Recycled Asphalt Mixes and their Pavement Performance. *Doboku Gakkai Rombun-Hokokushu/Proc. Japan Soc. Civil Eng.*, No. 1984(348), 1984, pp. 51-60.

23. Yamada, M. Recycled Asphalt Mixtures in Osaka and their Performance. *Memoirs of the Faculty of Engineering*, No. 28, 1987, pp. 197-201.

24. Goh, S. W., and Z. You. Mechanical Properties of Porous Asphalt Pavement with Warm Mix Asphalt and RAP. *Journal of Transportation Engineering ASCE*, No. 138, January 2012, pp. 90-97.

25. Shu, X., B. Huang, and D. Vukosavlijevic. Laboratory Evaluation of Fatigue Characteristics of Recycled Asphalt Mixture. *Construction and Building Materials*, No. 22(7), 2008, pp. 1323-1330.

26. Tao, M., and R. B. Mallick. An Evaluation of the Effects of Warm Mix Asphalt Additives on Workability and Mechanical Properties of Reclaimed Asphalt Pavement (RAP) Material.

Transportation Research Record: Journal of the Transportation Research Board, Vol. No. 2126, 2009, pp. 151-160.

27. Wen, H., and Y. R. Kim. Simple Performance Test for Fatigue Cracking and Validation with WesTrack Mixtures. *Transportation Research Record: Journal of the Transportation Research Board*, Vol. No. 1789, 2002, pp. 66-72.

28. Bukowski, J. Asphalt Pavement Recycling with Reclaimed Asphalt Pavement (RAP). September 16, 2011. http://www.fhwa.dot.gov/pavement/recycling/rap/index.cfm, Accessed 08/12, 2012.

29. Hoellen, K. Centering on Environmental Excellence. *Public Roads FHWA*, Vol. 67, No. 1, 2003, pp. August 10, 2012.

30. Huang, S. C. Rubber Concentration on Rheology of Aged Asphalt Binders. *Journal of Materials in Civil Engineering*, No. 20(3), 2008, pp. 221-229.

31. Huang, S.C., and Pauli, A.T. Particle Size Effect of Crumb Rubber on Rheology and Morphology of Asphalt Binders with Long-Term Aging. *Road Materials and Pavement Design*, No. 9(1), 2008, pp. 73-95.

32. Bahia, H. U., and A. F. Faheem. Using the Superpave Gyratory Compactor to Estimate Rutting Resistance of Hot-Mix Asphalt. *Transportation Research E-Circular*, 2007, pp. 45-61.

33. Hattingh, M. M. The Fractionation of Asphalt. *AATP*, No. 53-84, 1984, pp. 197-215.

34. Heitzman, M. State of the Practice-Design and Construction of Asphalt Paving Materials with Crumb Rubber. *Publication FHWA-SA-92-022*, 1992.

35. Gawel, I., R. Stepkowski, and F. Czechowski. Molecular Interaction between Rubber and Asphalt. *Industrial and Engineering Chemistry Research*, No. 45(9), 2006, pp. 3044-3049.

36. Billiter, T. C., and et. al. Physical Properties of Asphalt-Rubber Binder. *Petroleum Science and Technology*, No. 15(3-4), 1997b, pp. 205-236.

37. Airey, G. D., M. M. Rahman, and A. C. Collop. Absorption of Bitumen into Crumb Rubber using the Basket Drainage Method. *International Journal of Pavement Engineering*, No. 4(2), 2003, pp. 105-119.

38. Leite, L. F. M., and B. G. Soares. Interaction of Asphalt with Ground Tire Rubber. *Petroleum Science and Technology*, No. 17(9), 1999, pp. 1071-1088.

39. Behbahani, H., S. Nowbakht, H. Fazaeli, and J. Rahmani. Effects of Fiber Type and Content on the Rutting Performance of Stone Matrix Asphalt. *Journal of Applied Sciences*, No. 9(10), 2009, pp. 1980-1984.

40. Tayfur, S. H., H. Ozen, and A. Aksoy. Investigation of Rutting Performance of Asphalt Mixtures Containing Polymer Modifiers. *Construction and Building Materials*, No. 21(2), 2007, pp. 328-337.

41. American Association of State Highway and Transportation Officials. Standard Practice for Mixture Conditioning of Hot-Mix Asphalt. *AASHTO Designation R30-02*, 2006.

42. Texas Department of Transportation. Hamburg Wheel-Tracking Test. *TXDOT Designation: TEX-242-F*, 2009.

43. Witczak, M. W., K. Kaloush, T. Pellinen, M. El-Basyouny, and H. Von Quintus. Simple Performance Test for Superpave Mix Design. *NCHRP Report 465*, 2002.

44. Dongre, R., J. D'Angelo, and A. Copeland. Refinement of Flow Number as Determined by Asphalt Mixture Performance Tester: Use in Routine Quality Control - Quality Assurance Practice. *Transportation Research Record: Journal of the Transportation Research Board*, Vol. No. 2127, 2009, pp. 127-136.

45. Chong, K. P., and M. D. Kuruppu. New Specimen for Fracture Toughness Determination for Rock and Other Materials. *International Journal of Fracture*, Vol. 26, 1984, pp. R59-R62.

46. Ott, R. L., and M. Longnecker. An Introduction to Statistical Methods and Data Analysis, 5th Edition. , 2000.

47. Walls, J., and M. R. Smith. Pavement Division Interim Technical Bulletin, Life-Cycle Cost Analysis in Pavement Design - Interim Technical Bulletin. *FHWA-SA-98-079, U.S. Department of Transportation*, 1998.

48. Eurobitume. Life Cycle Inventory: Bitumen. , 2012.

49. Stripple, H. Life Cycle Inventory of Asphalt Pavements. , 2000.

50. Stripple, H. Life Cycle Assessment of Road: A Pilot Study for Inventory Analysis. , 2001.

51. Argonne National Lab, Energy Systems Division. Greenhouse Gases, Regulated Emissions, and Energy use in Transportation (GREET) Model. , 1999.

52. USEPA. NONROAD Model (Nonroad Engines, Equipment and Vehicles). , 2005.

53. USEPA. Compilation of Air Pollutant Emission Factors, Volume 1: Stationary Point and Area Sources, AP-42. *Fifth Edition*, Vol. 1, 1995.

54. Lecomte, M., F. Deygout, and A. Menetti. Emission and Occupational Exposure at Lower Asphalt Production and Laying Temperatures. , 2007.

55. USEPA. Tool for the Reduction and Assessment of Chemical and Other Environmental Impacts (TRACI). , 2008.

56. Marwa, H. Life-Cycle Assessment of Warm-Mix Asphalt: An Environmental and Economic Perspective. *Transportation Research Board 88th Annual Meeting*, 2009.

57. ISO. Environmental Management - Life Cycle Assessment - Principals and Framework, ISO 14040 Series. *1997*.

58. Lippiat, B. Building for Environmental and Economic Sustainability (BEES) Technical Manual and User Guide. , 2007.

59. Weiland, C. Life Cycle Assessment of Portland Cement Concrete Interstate Highway Rehabilitation and Replacement, Master Thesis. , 2008.

APPENDIX A

FHWA RealCost LCCA Software

Traffic Data

AADT at Beginning of Analysis Peiod (total both directions):	126500
Single Unit Trucks as Percentage of AADT (%):	1.58
Combination Trucks as Percentage of AADT (%):	5.22
Annual Growth Rate of Traffic (%):	4 ...
Speed Limit Under Normal Operating Conditions (mph):	55
Lanes Open in Each Direction Under Normal Conditions:	3
Free Flow Capacity (vphpl):	2128 ...

Free Flow Capacity Calculator 🖩

Queue Dissipation Capacity (vphpl):	1818 ...
Maximum AADT (total for both directions):	150000
Maximum Queue Length (miles):	3
Rural or Urban Hourly Traffic Distribution:	Urban ▼

Ok   Cancel

Value of User Time

Value of Time for Passenger Cars ($/hour):	18.7767 ...
Value of Time for Single Unit Trucks ($/hour):	30.1567 ...
Value of Time for Combination Trucks ($/hour):	36.5533 ...

Ok   Cancel

Traffic Hourly Distribution - Distribution 1

Distribution Name: Week Day 1

Hour	AADT Rural (%)	Inbound Rural (%)	Outbound Rural (%)	AADT Urban (%)	Inbound Urban (%)	Outbound Urban (%)
0 - 1	1.8	48	52	1.2	47	53
1 - 2	1.5	48	52	0.8	43	57
2 - 3	1.3	45	55	0.7	46	54
3 - 4	1.3	53	47	0.5	48	52
4 - 5	1.5	53	47	0.7	57	43
5 - 6	1.8	53	47	1.7	58	42
6 - 7	2.5	57	43	5.1	63	37
7 - 8	3.5	56	44	7.8	60	40
8 - 9	4.2	56	44	6.3	59	41
9 - 10	5	54	46	5.2	55	45
10 - 11	5.4	51	49	4.7	46	54
11 - 12	5.6	51	49	5.3	49	51
12 - 13	5.7	50	50	5.6	50	50
13 - 14	6.4	52	48	5.7	50	50
14 - 15	6.8	51	49	5.9	49	51
15 - 16	7.3	53	47	6.5	46	54
16 - 17	9.3	49	51	7.9	45	55
17 - 18	7	43	57	8.5	40	60
18 - 19	5.5	47	53	5.9	46	54
19 - 20	4.7	47	53	3.9	48	52
20 - 21	3.8	46	54	3.3	47	53
21 - 22	3.2	48	52	2.8	47	53
22 - 23	2.6	48	52	2.3	48	52
23 - 24	2.3	47	53	1.7	45	55
Total	100			100		

Restore Defaults   Ok

Added Time and Vehicle Stopping Costs ☒

Added Time per 1,000 Stops (Hours) | **Added Cost per 1,000 Stops ($)** | **Cost Escalation**

Initial Speed (mph)	Passenger Cars	Single Unit Trucks	Combination Trucks	Passenger Cars	Single Unit Trucks	Combination Trucks
0	0	0	0	0	0	0
5	1.02	0.73	1.1	3.942	13.505	49.0852
10	1.51	1.47	2.27	12.8918	30.2512	113.1354
15	2	2.2	3.48	22.1336	49.4794	189.7562
20	2.49	2.93	4.76	31.7404	70.664	277.4876
25	2.98	3.67	6.1	41.8582	93.3962	374.5484
30	3.46	4.4	7.56	52.706	117.1358	479.1866
35	3.94	5.13	9.19	64.3276	141.4448	589.6064
40	4.42	5.87	11.09	76.942	166.3962	704.0266
45	4.9	6.6	13.39	90.6222	189.9168	820.7244
50	5.37	7.33	16.37	105.5726	213.1016	937.9186
55	5.84	8.07	20.72	121.8662	234.8994	1053.7842
60	6.31	8.8	27.94	139.722	261.3108	1166.5254
65	6.78	9.53	31.605	159.1692	285.9264	1240.4744
70	7.25	10.27	39.48	180.4706	305.2276	1344.7038
75	7.71	11	47.9	203.7138	328.3102	1448.9332
80	8.17	11.73	57.68	229.001	351.3928	1553.1772

Cost Escalation

Base Transp. Component CPI: 231.317

Base Year: 2012

Current Transp. Component CPI: 231.317

Current Year: 2012

Escalation Factor: 1.00

[Escalate]

Idling Cost per Veh-Hr ($): 1.0113 | 1.1214 | 1.2042

[Restore Defaults] [Ok]

Alternative 1

Alternative: ◄ [**1**   ] ►

Alternative Description: [   ]   Number of Activities: [1 ▼]

Activity 1

Activity Description: [Control SMA   ]

Activity Cost and Service Life Inputs

Agency Construction Cost ($1000):	[69.9] ...	Activity Service Life (years):	[10] ...
User Work Zone Costs ($1000):	[ ] ...	Activity Structural Life (years):	[20] ...
Maintenance Frequency (years):	[5] ...	Agency Maintenance Cost ($1000):	[1] ...

Activity Work Zone Inputs

Work Zone Length (miles):	[1]	Work Zone Duration (days):	[2] ...
Work Zone Capacity (vphpl):	[1340] ...	Work Zone Speed Limit (mph):	[45]
No of Lanes Open in Each Direction During Work Zone:	[1]	Traffic Hourly Distribution:	[Week Day 1 ▼]

Work Zone Hours

	Inbound Start	End	Outbound Start	End
First Period of Lane Closure:	21	24	[ ]	[ ]
Second Period of Lane Closure:	0	5	[ ]	[ ]
Third Period of Lane Closure:	[ ]	[ ]	[ ]	[ ]

[Copy Activity]

[Paste Activity]

[Open...]   [Save...]   [Ok]   [Cancel]